Online Detection of Aggregation Processes Using Dielectric Spectroscopy

Christensen, Peter Vittrup

Publication date:
2009

Document Version
Publisher's PDF, also known as Version of record

ONLINE DETECTION OF AGGREGATION PROCESSES USING DIELECTRIC SPECTROSCOPY

PETER VITTRUP CHRISTENSEN

Section of Chemistry
Aalborg University
Ph.D. Dissertation, 2008

Printed in Denmark by
UNIPRINT, Aalborg University, June 2009
ISBN 978-87-90033-55-2

Preface

This dissertation is submitted in partial fulfilment of the requirements for obtaining the degree of doctor of philosophy (Ph.D.). The dissertation consists of abstracts in English and Danish, a short thesis, and four supporting papers.

The study was carried out at the Section of Chemistry, Department of Biotechnology, Chemistry and Environmental Engineering, Aalborg University during the period from February 2005 to July 2008 and was financed by Aalborg University. I wish to thank my supervisor Kristian Keiding for help and guidance, as well as Søren Hvidt (Roskilde University, Denmark) for helpful discussions and suggestions. Likewise, I wish to thank, Morten Lykkegaard Christensen, Mogens Hinge, Niels Peter Raj Andersen and Lisbeth Wybrandt for their encouragement, experimental assistance and many rewarding discussions. Finally, I wish to thank my wife Anne-Belle Rindel Olsen and my daughter Nanna for their love, support and patience.

Aalborg, October 2008

Peter Vittrup Christensen

LIST OF CONTENTS

Abstract

Flocculation is an important chemical unit operation often used as a pre-treatment before separation processes. To ensure optimal dosing of flocculants online methods capable of evaluating the extent of flocculation can be used. Presently, only few such methods exist and their use is limited to dilute suspension. As many industrial suspensions have high solid contents, new methods are therefore needed.

In this study the use of dielectric spectroscopy as a flocculation monitor has been investigated. A measurement cell was developed, which allows a continuous flow of sample to take place during measurement. Using dielectric spectroscopy the dielectric dispersions of the flocculated suspensions were measured. To examine the potential of the method, a selection of model compounds were synthesised and used in the flocculation experiments. From the measured dielectric dispersion the relaxation time and dispersion magnitude were extracted, and by comparing these to well-established methods for quantification of flocculation, their correlation to the flocculation process was evaluated.

Generally, the relaxation time was found to increase when aggregates were formed during the flocculation process. Thus, detection of flocculation was possible using dielectric spectroscopy. However, when aggregates of dense structure were formed, the changes in the relaxation time could not be directly related to the flocculation process. This problem was believed to occur due to the formation of structures with high relaxation times that could not been measured in the available frequency range. The magnitude of the dielectric dispersion also increased when aggregates were formed, but as it was also strongly dependent on particle and aggregate charge, its use for the evaluation of aggregation was found to be less effective as compared to the relaxation time.

The use of dielectric spectroscopy was found useful in monitoring aggregation processes. However, due to the limitations on the structure of the formed aggregates, the method is not applicable for all types of aggregation processes.

Dansk resume (Danish abstract)

Flokkulering er en vigtig kemisk enhedsoperation, der ofte anvendes som forbehandling inden separationsprocesser. Online målemetoder, der er i stand til at evaluere flokkuleringens omfang, kan anvendes for at sikre optimal dosering af kemikalier. I øjeblikket eksisterer der kun få sådanne metoder, og deres anvendelse er ofte begrænset til suspensioner med lave tørstofindhold. Da mange industri-suspensioner har en høj tørstofkoncentration, er der behov for nye metoder.

I denne afhandling er det undersøgt om dielektrisk spektroskopi kan anvendes som flokkuleringsmonitor. Til dette formål er der udviklet en målecelle, der tillader et kontinuert flow af prøve under målingen. Der er blevet syntetiseret en række modelstoffer til brug i flokkuleringseksperimenter for at undersøge metodens potentiale. Fra den målte dielektriske dispersion er relaksationstiden og størrelsen af dispersionen udledt. Ved at sammenligne disse med etablerede metoder til kvantificering af flokkulering, er deres korrelation med flokkuleringsprocessen blevet fastlagt.

Det blev fundet, at relaksationstiden generelt voksede når aggregater blev dannet gennem flokkuleringsprocessen. Ved brug af relaksationstiden er det derfor muligt at anvende dielektrisk spektroskopi til at detektere flokkuleringen. Når flokkuleringen førte til dannelse af kompakte aggregater kunne relaksationstiden dog ikke direkte relateres til flokkuleringsprocessen. Dette problem menes at opstå når de dannede strukturer i aggregaterne giver anledning til høje relaksationstider, der ikke kan måles i det frekvensområde, der er tilgængeligt for målingen. Det blev ligeledes fundet at størrelsen af den dielektriske dispersion voksede som konsekvens af aggregatdannelsen. Dispersionens størrelse var dog ligeledes stærkt afhængig af ladningen på partikler og flokke, og det blev derfor vurderet, at denne parameter var mindre anvendelig end relaksationstiden til at beskrive flokkuleringsprocessen.

Dielektrisk spectroskopi blev fundet anvendelig til at overvåge flokkuleringsprocesser. Grundet metodens begrænsninger på strukturen af de dannede aggregater kan den dog ikke anvendes til alle typer flokkuleringsprocesser.

1. Introduction

The term flocculation refers to the process where particles and macromolecules in the colloidal range (1 nm to 1µm) form aggregates due to the addition of chemicals. Often the use of the term flocculation is reserved for aggregation processes where polymeric substances are used, but in this study it will be used to describe the formation of aggregates independent of the chemical in use. Flocculation is an important unit operation often used before separation processes such as filtration, sedimentation, centrifugation and flotation. The process is used in several industries; e.g. in pharmaceutical industries where flocculation for examples improves the separation of insulin from the producing microorganisms, in paper mills where flocculation improves the dewaterability and stability of the paper and in mining industries where flocculation aids the dewatering of inorganic slurries. The process also has many environmental applications such as improvement of sludge dewatering in waste water treatment and improvement of drinking water quality in water works.

The use of flocculation as a pre-treatment step is often critical for the performance of the separation process [1-4]. Aggregation of particles into flocs improves separation i.e. higher quality of the liquid phase (in terms of purity) and increased capacity of the separation equipment. During the separation process the suspension is exposed to a certain level of mechanical stress. This stress may destroy the weak flocs in the suspension and lower the efficiency of the separation. Flocs formed by the flocculation process often possess high mechanical strength, but the process also improves the strength of naturally occurring weak flocs, thus rendering the suspension less sensitive to mechanical stress.

Generally, flocculation processes are divided in to four subgroups categorised by the main mechanism responsible for the formation of the aggregates. These four are 1) shielding of charge, 2) neutralisation of charge, 3) formation of electrostatic patches and 4) formation of inter-particle bridges [5].

As charges on particles and macromolecules are often the most important factor for their stability, a shielding of these charges by addition of ions reduces their stability. Increasing the ionic concentration reduces the thickness of the electric double layer and decreases the electrostatic potential from the charges at a given distance from the particle.

This process is sometimes referred to as coagulation. When the electrostatic repulsive forces are sufficiently reduced, coagulation occurs due to the dominance of the attractive van der Waals forces. The formed aggregates are often very weak, due to the small net attractive force [5].

Charge neutralisation occurs when the adsorption of ions or polymers partly neutralises the charges on the particle or macromolecule. If the adsorption is evenly distributed on the surface, a homogeneous reduction in the charge takes place. This lowers the repulsive electrostatic forces between the particles, and once the charge is sufficiently reduced, the attractive van der Waal forces dominate and small, weak aggregates are formed [6].

Flocculation through the formation of electrostatic patches takes place when a polymeric flocculant comparable in size to the particle, but of opposite charge, is used. This may result in adsorption on the particle surface in a mosaic pattern. If the distance between charges on the polymer is less than the distance between the surface charges on the particle, patches of opposite charge as the particle form on the surface. The interaction between these patches and free areas of other particle surfaces adds an electrostatic contribution to the attractive van der Waal forces, making the resulting aggregates much stronger than aggregates formed solely by charge neutralisation [7]. The larger attractive forces between the particles also increases the collision efficiency and thereby results in more open aggregate structures as the particles do not need to configure in a compact structure to increase the number of contact points [5].

Flocculation by the formation of inter-particle bridges occurs when large polymers exceeding the size of the particle are used. These polymers may adsorb to several particles and thereby form bridges between them. The resulting aggregates often have an open structure, as the particle separation is relative large due to the polymer bridges. This type of flocculation may take place even though the surface charge of the particles is only slightly reduced [5].

The fundamental mechanisms of the flocculation process have been the subject of several studies during the last decades [8-23], and many of the aspects of the process are now well understood. Despite this improved insight, it is still difficult to predict the optimal type of flocculation chemical and the dosages needed to obtain optimal flocculation from the

physico-chemical properties of the feed. Furthermore, information of these properties is seldom available for industrial suspensions. The problems with the prediction of the outcome of the process arise partly due to the complex interaction and interdependence of several sub-processes involved in the flocculation and partly due to the broad distribution of particle properties often found in such suspensions. Thus, optimisation of chemical type and dose must be evaluated be assessing the effect of the addition.

Investigations of chemical choice and dosage are normally carried out in small scale experiments where supernatant clarity after sedimentation is used to evaluate the quality of the flocculation process. This type of experiment is often referred to as jar tests. Even though such an approach may be useful as a guideline for improving the industrial process, it is unfit for optimisation of flocculation for several reasons. When scaling the laboratory results, factors such as mixing of chemicals into the suspension, shear stresses in pipes and pumps, and size of turbulent eddies are difficult to take into account. Furthermore, in an industrial plant, flocculation often takes place as a continuous process in the sense that flocculation chemicals are continuously added to a flowing suspension. Variations in parameters such as particle concentration, pH, ionic strength and temperature of the suspensions are likely to occur due to variations in the production. This will influence the flocculation process and make a predetermination of chemical dosage difficult. Finally, the objective of the flocculation process could be to optimise e.g. flotation properties or filterability and not necessarily to improve the sedimentation properties, which is the criterion of quality in the jar test. This may result in the optimisation of the wrong floc properties.

To solve such problems an on-line measurement to evaluate the state of flocculation is needed. In this context on-line denote a continuous and in situ measurement. Fig. 1 shows a schematic diagram of how such a measurement could be implemented into to separation process.

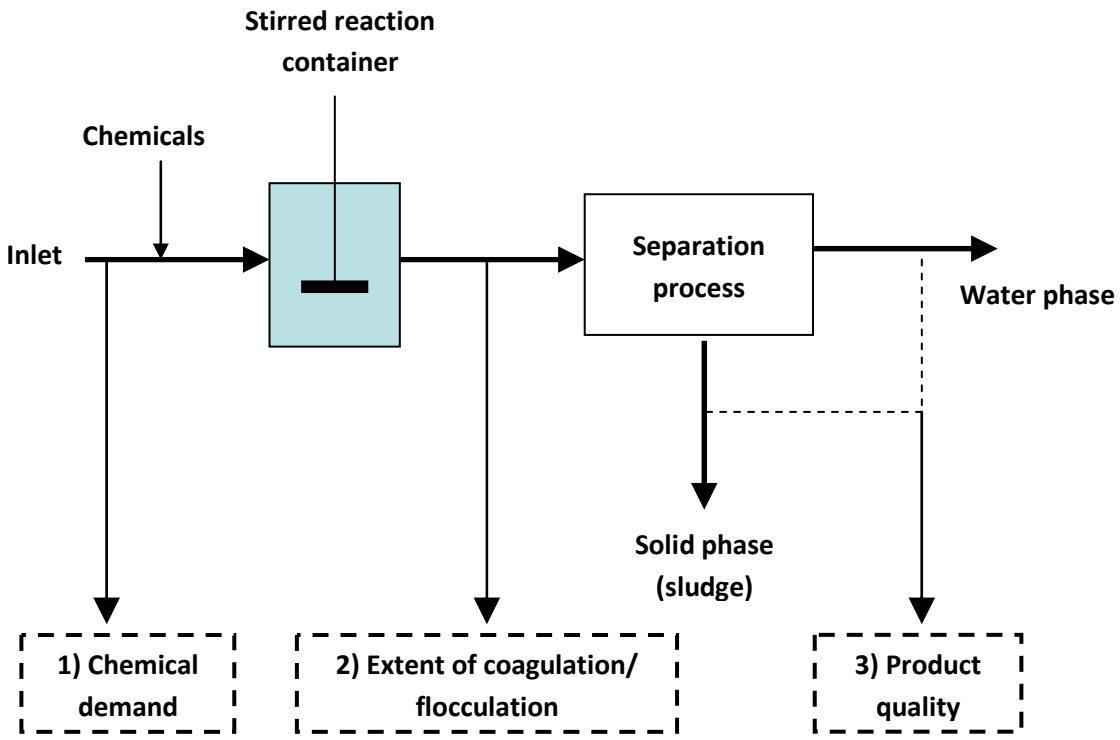

Fig. 1. Schematic drawing of the flocculation and separation process. The possibility of introducing measurements before and after the chemical addition as well as after the separation process is indicated.

Measurements can be made 1) prior to the point of chemical dosing which can be used to predict the dosage, e.g. particle concentration or charge. 2) after the point of chemical dosing, which evaluate the state of flocculation, e.g. floc size, floc structure or floc charge. 3) after the separation process and thereby evaluate separation quality on either the retentate or the permeate, e.g. turbidity, retention coefficients, water content of solid fraction. Measurements before dosing (1) require a model to predict the dosage, which is only rarely available. Measurement after the separation (3) is the most direct way of assessing the influence of the flocculation process on the separation, but due to the time delay between dosage and measurement it is only usable if the feed composition changes slowly compared to this delay time. Furthermore, such measurements are not able to reveal whether a reduction in separation quality originates from the flocculation process or a mechanical error occurring in the separation process itself. Measurement before separation (2) provides direct assessment

of the effect of the chemical dosage with low time delay, and is the most effective way of monitoring the flocculation process.

The need of an on-line measurement for the evaluation of flocculation has brought about a number of studies on the subject, and several techniques have been investigated for their potential use in this context. In the following the most important of these techniques usable for measurement after chemical dosing will be briefly described.

1.1 Photometric dispersion analyser

The photometric dispersion analyser, PDA, is an optical technique utilising the local fluctuations in particle density in a flowing suspension. A beam of light is used to illuminate the suspension flowing in a transparent tube, and the intensity of the transmitted light is measured. As the illuminated volume is small, the particle concentration is not completely constant over time, which results in fluctuations in the transmitted light. The magnitude of the observed fluctuations is dependent on the length scale of the illuminated volume and the particles, and thus larger particles results in larger fluctuations [24]. This can be utilised when assessing the state of flocculation as the formation of particle aggregates greatly increases the magnitude of the fluctuations. Denoting the average intensity of transmitted light *DC* and the root mean square of the deviation from this value *RMS,* a useful index of flocculation can be defined:

$$RATIO = \frac{RMS}{DC} \qquad \text{Eq. [1]}$$

This index, termed *RATIO,* is almost unaffected by fouling of the optical tube and is significantly increased as flocculation occurs.

Although proven to be a powerful tool for characterising flocculation processes, the technique has two limitations that make it difficult for use in some industrial applications. Due to the requirement of transmittance of light through the suspension the particle concentration must be fairly low. In a study by Li and Gregory [25] flocculation of kaolin particles was investigated and it was found that the PDA was able to monitor the process up to a particle volume fraction of 1.2%. For polystyrene particles, the concentration has to be below 1% to obtain useful data [26]. This limit may be increased by decreasing the diameter

of the tubing thus allowing more light to be transmitted. However, this will be on the expense of worsening the other already existing problem of the technique. As the illuminated volume needs to be small, a transparent tube of 3 mm in diameter is normally used. The flocs created in many flocculation processes are comparable to this size, if not larger. Flocs larger than the tube diameter will be destroyed when passing the tube and even flocs considerably smaller are likely to deflocculate due to the increased shear forces in the narrow tube. Therefore, the benefit on maximum particle concentration gained by using a smaller tube will lower the maximum floc size allowed to pass undisturbed. If the formed aggregates are broken down during their passage through the tube the measurement will not resemble the actual state of flocculation and will thus be misleading and unsuitable for monitoring the process.

1.2 Streaming current detector

The streaming current detector (SCD) was first developed by Gerdes [27] and gives a signal that correlates with the charge of the particles in a suspension. Even though not a direct measure of flocculation, the particle charge is often the most important suspension property in determining how stable the suspension is, and it is therefore possible to use it as an indicator of whether flocculation is likely to occur. The technique is based on a piston moving up and down in a cylinder thus causing a well defined movement of the suspension along the walls of the cylinder and piston. During the measurement, particles present in the suspension will momentarily adsorb to the surface of either the cylinder or the piston, and the movement of the suspension relative to the particles will cause a movement of the counter-ions in the electric double layer of the particles. This transport of charge away from its counter charge on the particle surface induces what is termed a streaming current, which increases with particle charge. The technique is more thoroughly described by Dentel and Kingery [28].

SCD is being used to control the chemical dosing in several water works in the US and has helped reduce the chemical dosing by 12% in average [29]. In Denmark it is presently being used on-line to control flocculation processes at waste water treatment plants.

Despite its usefulness in several applications this technique is also limited to fairly low particle concentrations, and in most published experimental setups using this method, particle concentrations in the range 0.3-2 g/L are used [28,30-32].

Another aspect of the SCD that has been questioned is its capability to provide a representative measure of particle charge. As the condition for contribution of a particle to the measurement is adsorption, all particles types present may not necessary contribute equally due to differences in adsorption affinity [33]. Furthermore, incomplete coverage of the cylinder and piston surfaces will result in a decrease in the induced streaming current thus rendering the result difficult to interpret [33]. Studies have also shown that the surfaces of the cylinder and the piston themselves contribute to the measurement resulting in a non-zero offset of the streaming current [28].

1.3 Turbidity measurement

The turbidity of a suspension arises from the scattering of light by the suspended particles. The amount of scattered light depends on both particle size and concentration [34]. The dependence of the turbidity on particle size is determined by the wavelength of the light in relationship to the particle size as described in the Mie scattering theory. This principle was used by Jeffrey and Ottewill [35] in a study of salt induced coagulation of polystyrene particles. By measuring the turbidity (t_1 and t_2) of the suspension at two different wavelengths (λ_1 and λ_2) they computed a function T which was used as a relative measure of particle size.

$$t_R = \frac{t_1\lambda_1}{t_2\lambda_2} \qquad \text{Eq. [2]}$$

Salt-induced coagulation caused a marked decrease in T due to the formation of larger aggregates. However, care has to be taken when selecting the wavelengths at which the turbidity was measured as a minimum in T as a function of particle size can occur. Thus, observed changes in turbidity can be difficult to relate to an aggregation process as both an increase and a decrease in T may result, depending on the combination of selected wavelengths and the size of the particles in the suspension. Furthermore, the measurement of turbidity requires some transmittance of light through the sample and thus limits the application of this method to fairly dilute suspensions.

1.4 Image analysis

During the last decade, the improvement in the quality of high resolution cameras and the increased computational capacity of computers have made on-line image analysis of aggregates possible. In general image analysis consists of two steps; 1) acquirement of a picture of the aggregates and 2) analysis of the picture by use of a mathematical algorithm. Although the general principal is the same, several approaches have been used to deal with these two steps. Tang *et al*. obtained pictures of polystyrene particle aggregates with a camera connected to a microscope and analysed them in terms of fractal dimensions [36]. Using a high speed camera and Fast Fourier Transformation Analysis of the pictures, Wågberg and Ericksson monitored the flocculation of cellulosic fibres [37]. The pictures were taken of the fibre suspensions flowing through a narrow channel (3 mm) in a transparent glass block. More recently Kilander *et al*. used particle image velocimetry to obtain aggregate pictures from a suspension of kaolin [38]. The pictures were analysed by a connected component labelling technique.

Although image analysis has proven useful for characterising the flocculation process in several different types of suspensions its use seems limited to semi-dilute suspensions as the particle concentrations used in the above mentioned studies were 5 g/L for the cellulosic fibres and below a volume fraction of 0.1% for the two studies of colloidal suspensions.

1.5 Rheology

The use of rheological measurements for the study of suspension structure is widespread, and in several studies the effects of flocculation on rheological parameters have been examined [39-42]. However, only a limited number of studies have investigated the potential of using rheological measurements for on-line evaluation of flocculation process [43,44]. These studies are mainly focussed on the flocculation of sludge and use the curve shape in the rheogram (shear stress versus shear rate) to assess the influence of polymer dosage on the state of flocculation. At low polymer dosage the shear stress increased as a function of shear rate, but at higher dosages a peak in the shear stress was observed. Although the occurrence of this peak is a consequence of the polymer induced flocculation, Abu-Orf

and Dentel [44] found no correlation between optimal polymer dosages and the height of the peak. Thus, changes in the rheological properties of a suspension can be measured during flocculation, but a relation between the observed changes and the optimal flocculant dosage has not been established.

1.6 The need of alternative techniques

Several techniques which can be used to obtain an on-line evaluation of a flocculation process exist as shown in the previous sections. However, they are generally limited to dilute suspensions which restrict their use in industrial applications where suspensions of high solids content are often found. As discussed earlier, other features of the individual techniques may also limit their use in large scale productions. Although the available techniques are able to provide valuable information on flocculation and are fully capable of monitoring and controlling the process within some areas, there are still some aspects of the process itself and several areas of application, e.g. high solid concentration suspensions, which they do not cover. Thus, new techniques which may complement the existing are needed. A potential technique in this context is dielectric spectroscopy (DS). Using measurements the dielectric properties of a suspension is probed as a function of electric field frequency. The obtained spectrum holds information of dielectric relaxation processes within the suspension which in some case are related to particle characteristics. This technique has been used to characterise colloidal suspensions for several decades. During this period, several studies have shown that it is possible to obtain knowledge on both particle size and charge from the measurement [45,46]. As these are the two most important suspension properties in relation to flocculation, DS has the potential to be used to study the process. Furthermore, the technique can be used at high particle concentrations and suspensions of particle volume fraction as high as 0.3 have successfully been characterised [47]. Although it seems that DS possesses the essential properties needed for evaluating flocculation processes, studies of its use within this area are peripheral. For these reasons the use of DS in monitoring flocculation process will be investigated in this thesis.

2. Objective

In the introduction the need of new techniques for evaluating the state of flocculation in particle suspensions was pointed out, and the potential use of DS for such applications was justified. This technique has previously been used to characterise single colloidal particles but not the aggregation of these. The objective of this thesis is therefore to investigate the possibility of using DS for monitoring flocculation process. The long term aim of this work is the implementation of DS as a flocculation monitor in a real industrial process, but as this exceeds the time frame of this thesis, an intermediate aim has been set up. Thus, it has been chosen the focus on the flocculation of well characterised model systems where the identification of cause and effect is easier accessible. From the conclusions obtained through these model systems and assessment of the potential of DS as a flocculation monitor will be given. Thus, the objectives of this thesis can be stated as:

- Design and construction of a DS measurement cell appropriate for use in an on-line evaluation of a flocculation process.
- Evaluation of flocculation processes of model particles and macromolecules using DS.
- Assessment of the potential of DS as an on-line flocculation monitor.

3. Experimental approach

In this chapter the experimental approach is described. An investigation of the potential of DS to characterise flocculation processes could be carried out in several ways dependent on the specific area of interest. Below three such approaches are described.

- A number of suspension batch samples are flocculated using different flocculant dosages. These are then transferred to the DS measurement cell one by one, and the dielectric spectra of the samples are measured.
- A single suspension batch is gradually flocculated by stepwise addition of flocculant. The suspension is continuously pumped from the batch to the DS measurement cell for measurement of the dielectric spectrum and back to the batch.
- A suspension is pumped through the DS measurement cell without recirculation. Flocculated is induced by a continuous addition of flocculant to the suspension stream prior to the entry into the measurement cell.

The sequence of the three approaches represents an increasing degree of resemblance to an industrial flocculation process. Although it is the objective to investigate the potential use of DS as a flocculation monitor in a ‘real’ process, several other factors apart from the resemblance of industrial conditions needs to be considered. As the production of model particles and macromolecules are time consuming processes (synthesis and cleaning) and the available product mass is limited by the size of the synthesis setup, the use of large quantities of the model suspensions is not practically possible. Thus, the third approach is not feasible as large volumes of suspension are required for this setup. This problem is avoided in the second approach due to the recirculation if the suspension. However, in this setup the flocculation process itself does not resemble an actual process accurately, as the flocculant is added gradually over a long period of time. Due to the importance of kinetics in many flocculation processes this may potentially result in altered flocculant consumption and flocculation mechanism as compared to an instantaneous dosage of flocculant. Although an important issue from a kinetic point of view, this is considered a

secondary problem in this study as the purpose is to investigate to potential of using DS to characterise the process of flocculation in general. The problem of gradual addition of flocculant is solved in the first approach due to the instantaneous dosing. However, this approach involves other problems which are considered more critical. The effect of the suspension flowing through the measurement cell is not investigated in this setup. Furthermore, due to the considerable time needed to conduct the measurement of the dielectric spectrum aggregates formed by the flocculation process may sediment during the experiment, thus changing the result. If the suspension were to be re-circulated during the measurement a much larger volume would be needed, and due to the number of batches this would require an unrealistic amount of model material. For these reasons the second approach has been chosen as it is considered the optimal compromise between what resembles an industrial process and what is practically attainable.

3.1 Model systems

When investigating the potential use of DS as a monitor for flocculation processes it is necessary to keep in mind the diversity of both the starting point (the suspension) and ending point (the aggregates) as well as the large difference between the two. This is important as the DS measurement must be able to register both the components of suspension and the formed aggregates to properly assess the flocculation process. Suspensions found in ‘real’ systems are often a complex mixture of aggregated material, colloidal particles, dissolved macromolecules, and various ions. Apart from this, the large variety in the composition of these components makes it impossible to select or create a representative suspension that generally reflects the composition and properties of ‘real’ suspensions. Furthermore, the properties of the formed aggregates vary considerably in terms of size, compactness and shape, thus a generalisation of the aggregate properties is not possible either. Therefore, conclusions made from one flocculation process do not necessarily comply with others, and thus it is difficult to study the flocculation process in generalised terms. For this reason it has been chosen to use model systems to investigate the flocculation process in this study. Although the use of model systems does not solve

the problem of conducting representative experiments of the flocculation process in general, it holds the opportunity of investigating the effects of fundamental suspension properties on the process. In this study three types of model components have been chosen to represent the constituents of ‘real’ suspension. In the following these model components are presented along with the chemicals that will be used to flocculate them. The expected properties of the resulting aggregates are also discussed. In Fig. 2 the used model components and the expected resulting aggregates are schematically illustrated.

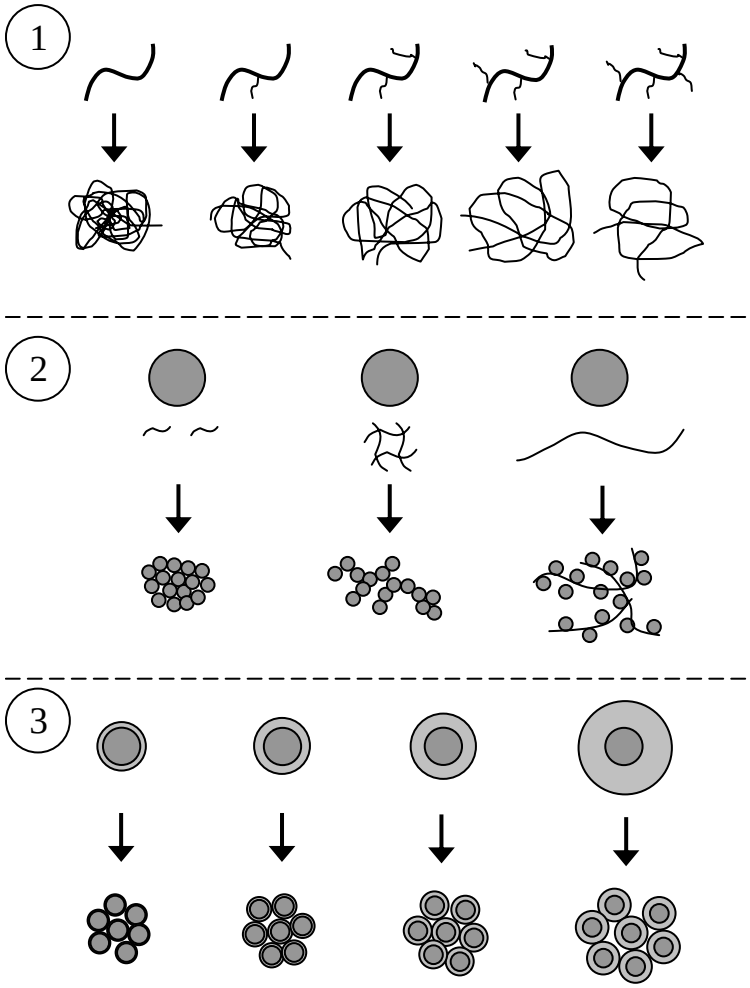

Fig. 2. Schematic drawing of the model colloids used in this study. The aggregates resulting from the flocculation of these compounds is also shown. 1) Hydrophobically modified poly(acrylic-acid). 2) Polystyrene particles and different flocculants. 3) Core-shell particles.

3.1.1 Hydrophobically modified poly(acrylic-acid) polymers

These model components consist of polymers of acrylic acid with a molecular mass of 100 kDa. Using dodecylamine (a C-12 chain) a varying fraction (X%) of the carboxylic groups were modified with a hydrophobic side chain. Five polymers with a modification degree of 0, 1, 3, 6 and 8% were made and they are referred to as HMPAA-X.

The hydrophobically modified polymers are used to represent dissolved macromolecules (e.g. proteins and humic acids), which are large, charged molecules with some hydrophobic segments. These polymers are aggregated using barium ions. The formation of chelates between the barium ion and the carboxylic acid groups decreases the solubility of the polymer and thereby result in the formation of aggregates. Barium was chosen due to its negligible formation of hydroxide and carbonate species as compared to e.g. calcium, iron and aluminium. In this way it is ensured that all the barium is dissolved as Ba^{2+} and available for complexation with the carboxylic acid. Furthermore, the use of barium for the precipitation of poly(acrylic-acid) has previously been studied [48,49], so that a frame of reference exists for this system. The degree of hydrophobic modification is expected to affect the degree of charge neutralisation needed to precipitate the polymers. Furthermore, the presence of hydrophobic side chain is expected to result in a more open aggregate structure, partly because of the steric hindrance of the chains and partly due to a higher degree of un-neutralised charges remaining at the point of aggregation.

3.1.2 Polystyrene particles

The polystyrene particles are hard, spherical particles with a negative surface charge. They are monodisperse with a diameter of approximately 370 nm. This type of particles has been used extensively in studies of flocculation processes [7,11,15,18,19,22,50].

These particles are used to represent hard, colloidal particles (e.g. inorganic particles) which generally carry a negative charge under natural conditions. These particles are flocculated using three different types of cationic polymers.

1) A small, linear, highly charged polymer, poly(DADMAC). Flocculation using this polymer is expected to be caused by charge neutralisation. This results in compact flocs due to a low collision efficiency.
2) A large, linear, low charged polymer, Zetag 7633. Flocculation using this polymer is expected to be caused by formation of inter-particle bridges, and thus result in open flocs possibly without contact between the particles.
3) A cross-linked, low charged polymer, Zetag 7867FS40. Flocculation using this polymer is expected to be caused by formation of electrostatic patches. This results in open flocs due to a high collision efficiency.

3.1.3 Core-shell particles

These particles consist of a solid polystyrene core and a water swollen shell of poly(acrylic acid) chains extending from the surface of the core. Particles with different acrylic acid (AA) contents resulting in different shell thicknesses (3-285 nm) are used. The particles are denoted 11%AA, 19%AA, 37%AA and 54%AA referring to their molar content of acrylic acid. They represent colloidal particles covered by polymeric substances (e.g. bacteria) which generally carry a negative charge under natural conditions. These particles are flocculated using two cationic polymers which differ only in their molecular weight. The smaller is referred to as LMW whereas the larger is denoted HMW. Both of them are low molecular weight (compared to traditional flocculants), highly charged polymer expected to result in the formation of compact aggregates. However, as only the outer charges of the particles need to be neutralised before flocculation can occur, the shells of the aggregated particles are expected to be partly water swollen and carry a substantial amount of charge.

It is important to state that the model systems have not been chosen to mimic the exact composition and properties of ‘real’ suspensions, but instead to resemble a broad range of the components that may be found in the suspensions. Furthermore, the model systems have been designed in a way that is believed to result in the formation of aggregates with a wide variety of properties. This array of model systems makes it possible

to investigate the capability of DS to monitor flocculation processes of different suspensions components into aggregates with varying properties. In this way the usability of the method can be assessed in terms of basic properties of the suspension and the aggregates.

3.2 Setup for flocculation experiments

In the chosen experimental setup the suspension is pumped through the DS measurement cell and back to a flocculation chamber in which the flocculant is dosed gradually. The measurement cell itself and the measurement of the dielectric spectrum will be discussed later in section 4.4. The flocculation chamber is constituted of a glass beaker placed in a temperature controlled water bath. The suspension or solution is stirred to ensure mixing of the added chemicals. A schematic drawing of the experimental setup can be seen in Fig. 3. A PDA apparatus in series with the DS measurement cell has been included in the figure, but is only used in some experiments.

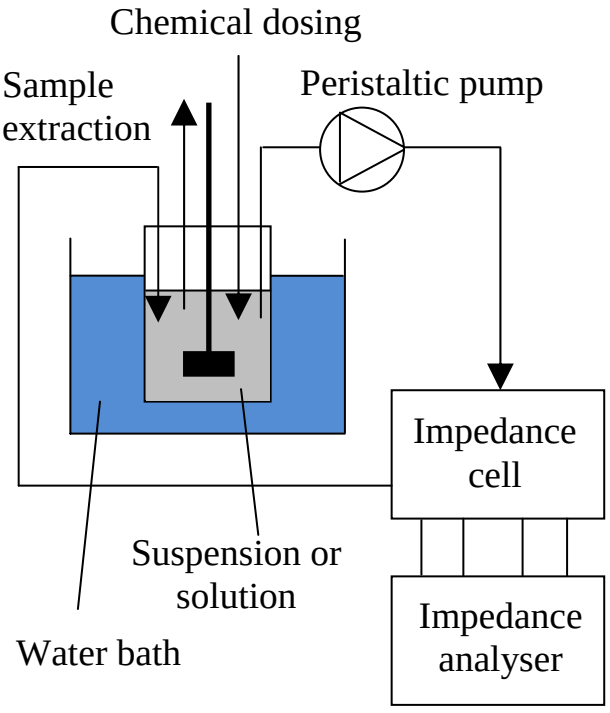

Fig. 3. Experimental setup used in the flocculation experiments.

3.3 Reference methods

Apart from the measurement of the dielectric spectrum the flocculation process is characterised by a reference method. In the following these are briefly described.

3.3.1 Photometric dispersion analyser

When the suspension turbidity allows it (i.e. is sufficiently low) a PDA2000 (Rank Brothers Ltd) is used for the evaluation of the state of flocculation. The apparatus is placed in series with and prior to the DS measurement cell. A transparent tube with a diameter of 3 mm is used. In each experiment the *DC* gain and *RMS* gain settings are adjusted to maximise the utilisation of the signal output range (0-10 V) and thereby achieve the optimal resolution on the data. To ease the comparison of the data independent of the gain settings used a normalised *RATIO* value ($RATIO_R$) is used:

$$RATIO_R = \frac{RATIO - RATIO_{min}}{RATIO_{max} - RATIO_{min}} \qquad \text{Eq. [3]}$$

where the subscripts min and max refers to the minimum and maximum value of the *RATIO* signal in the experiment.

3.3.2 Residual turbidity

When suspensions of high particle concentrations are used, the degree of flocculation is determined by the residual turbidity after centrifugation. By submitting the suspension to a centrifugation force, particles and flocs below a limiting size are removed and the residual turbidity of the supernatant can be determined. The size limit is determined by the applied centrifugation force and time and can be estimated using Stokes' law. This method allows a determination of the fraction of small particles and flocs and can be used to evaluate the extent of flocculation.

3.3.3 Electrophoretic mobility and size

As a supplement to these methods, in some experiments measurements of electrophoretic mobility and floc size are made. This is done on diluted samples taken from the flocculation chamber during the experiment using a Zetamaster S (Malvern Instruments) and a Microtrac II particle size analyser (PSA) (Leeds & Northrup).

4. Dielectric spectroscopy

In this chapter the principle of DS and its use in colloidal science will be discussed. Furthermore a description of dielectric measurements and analysis is given. Finally the experimental procedure used to obtain the dielectric spectrum in this work is evaluated.

4.1 The principle of dielectric spectroscopy

The dielectric properties of a material are often given as the static relative permittivity (ε). This value is a measure of the material's ability to polarise in an electric field. The polarisation may take place due to an orientation of polar molecules in the material or a displacement of charge inside a structural component in the material. However, as the polarisation process is not infinitely fast, the static relative permittivity is only obtained if sufficient time is available for the material to completely polarise. Thus, if applying an alternating electric field to the material the permittivity will depend on the frequency of the field. When the frequency increases the time available for polarisation decreases and at a certain frequency insufficient time is available for the material to polarise, thus reducing the permittivity significantly. Typically the decrease will take place over a frequency range spanning approximately one order of magnitude, and at frequencies above or below this region the value of the permittivity is almost constant. This inability to remain polarised in the field is termed a relaxation of the material and the change in permittivity is termed a dielectric dispersion. The characteristic time of the relaxation process is called the relaxation time (τ). Several polarisation processes may take place in a material and their respective relaxation times can differ by many orders of magnitude. The polarisation time of a molecule or structure generally depend on the size, as larger molecules or structures polarise slower than smaller ones. However, several other factors such as temperature, interaction with other molecules/structures, presence of ions etc. may have significant effects on τ as well.

The polarisation of a material results in a loss of energy due to the movement of ions or molecules. If the frequency of the electric field is comparable to the characteristic frequency of the relaxation (τ^{-1}) the energy loss will be large as the time between each re-orientation is small. At lower frequencies the fraction of the oscillating period of the field in which the polarisation takes place is small and thus the energy loss tends towards zero. At higher frequencies the energy loss tends towards zero as well due to the lack of polarisation. The energy loss appears as an imaginary part in the relative permittivity thus making it a complex quantity (ε*) which can be written as:

$$\varepsilon^* = \varepsilon' - i\varepsilon'' \qquad \text{Eq. [4]}$$

The real part (ε') is the normal relative permittivity and the imaginary part (ε'') is denoted the dielectric loss. The two components of the complex relative permittivity are inter-related through variation in the angular frequency (ω) by the Kramers-Kronig relation [51].

From the measurement of the dielectric spectrum and the relaxation processes, knowledge about a wide range of material properties can be obtained and for this reason the technique has been used within many areas of research e.g. biological cells [52-54], micellar structure [55], polymers solution [56,57], biofilms [58], blood coagulation [59], membrane characterisation [60].

4.2 Colloidal characterisation by dielectric spectroscopy

When a colloidal suspension is exposed to an oscillating electric field, changes in the permittivity as a function of frequency occur. These changes, which are called dielectric dispersion, are caused by relaxation processes that are related to the properties of the colloids and the medium in which they are suspended. In the following the relaxation processes found in colloidal suspensions and their significance in colloidal characterisation are described.

4.2.1 Maxwell-Wagner relaxation

In a particle suspension the dielectric and conductive properties of the medium and the disperse phase often differ. In an electric field the transport of charge in the medium towards the particle surface is determined by the field in the medium (E_m) and the conductivity of the medium (K_m) as the current density (i_m) can be expressed as:

$$i_m = E_m K_m \qquad \text{Eq. [5]}$$

As the relative permittivity of the medium (ε_m) is defined as the factor by which the medium reduces the field as compared to the field in vacuum (E_0), Eq. [5] can be rewritten as:

$$i_m = \frac{E_0}{\varepsilon_m} K_m \qquad \text{Eq. [6]}$$

Inserting the conductivity (K_p) and relative permittivity (ε_p) of the particle into Eq. [6] an expression for the current density inside the particle (i_p) is obtained. If the current densities inside and outside the particle are different, charge will built up on both sides of the particle and create a dipole that gives rise to an increase in the permittivity of the suspension. This occurs when the inequality in Eq. [7] is satisfied, which is practically always the case:

$$i_m \neq i_p \Leftrightarrow \frac{E_0}{\varepsilon_m} K_m \neq \frac{E_0}{\varepsilon_p} K_p \Leftrightarrow \frac{K_m}{\varepsilon_m} \neq \frac{K_p}{\varepsilon_p} \qquad \text{Eq. [7]}$$

This effect was first described by Maxwell [61] and later extended by Wagner [62,63]. Thus, the relaxation process is termed the Maxwell-Wagner (MW) relaxation. The magnitude and the relaxation time of the MW relaxation of a suspension with a particle volume fraction of ϕ can be determined as [64]:

$$\Delta\varepsilon_\mathrm{MW} = \frac{9\left(\varepsilon_\mathrm{m} K_\mathrm{p} - K_\mathrm{m}\varepsilon_\mathrm{p}\right)^2 \phi\left(1-\phi\right)}{\left[\varepsilon_\mathrm{p}\left(1-\phi\right)+\varepsilon_\mathrm{m}\left(2+\phi\right)\right]\left[K_\mathrm{p}\left(1-\phi\right)+K_\mathrm{m}\left(2+\phi\right)\right]^2} \qquad \text{Eq. [8]}$$

$$\tau_\mathrm{MW} = \frac{\varepsilon_0\varepsilon_\mathrm{p}\left(1-\phi\right)+\varepsilon_0\varepsilon_\mathrm{m}\left(2+\phi\right)}{K_\mathrm{p}\left(1-\phi\right)+K_\mathrm{m}\left(2+\phi\right)} \qquad \text{Eq. [9]}$$

For a charged particle the high concentration of counter-ions close to the particle surface results in an increased conductivity referred to as surface conductivity. The surface conductivity (K^{σ}) can be split into two contributions; one arising from the diffuse part of the double layer (K_{d}^{σ}) and one from the inner part of the double layer (Stern layer) (K_{i}^{σ}). The contribution from the diffuse part can be determined using the Bikerman equation [65].

$$K_{\mathrm{d}}^{\sigma} = \frac{2K_{\mathrm{m}}}{\kappa}\left(\frac{D^{+}}{D^{+}+D^{-}}\left[\exp\left(-\frac{ze\zeta}{2k_{\mathrm{B}}T}\right)-1\right]\left(1+3m^{+}\right) + \frac{D^{-}}{D^{+}+D^{-}}\left[\exp\left(\frac{ze\zeta}{2k_{\mathrm{B}}T}\right)-1\right]\left(1+3m^{-}\right)\right) \qquad \text{Eq. [10]}$$

where D^{+} and D^{-} are the diffusion coefficients of the cation and anion respectively, z is the ion valency, e is the elementary charge, ζ is the zeta potential, k_{B} is the Boltzmann constant, T is the temperature, κ^{-1} is the Debye length, η is the medium viscosity and

$$m^{\pm} = \frac{2\varepsilon_{\mathrm{m}}}{3\eta D^{\pm}}\left(\frac{k_{\mathrm{B}}T}{ze}\right)^{2} \qquad \text{Eq. [11]}$$

The contribution from the stagnant layer is not readily attainable from the physical properties of the suspension, as is the case for K_{d}^{σ}, instead it is described through the parameter θ which is defined as:

$$\theta = \frac{K_{i}^{\sigma}}{K_{d}^{\sigma}} \qquad \text{Eq. [12]}$$

The surface conductivity increases the total conductivity of the particle markedly and O'Konski [66] showed that by assuming that conductivity contribution of the particle itself is negligible compared to the surface conductivity, K_{p} in Eq. [8] and Eq. [9] should be substituted by $2K^{\sigma}/a$, where a is the particle radius. This type of modified MW relaxation is termed the Maxwell-Wagner-O'Konski relaxation (MWO). For the polystyrene particles used in this study this relaxation should be found at frequencies around 500 kHz which is in the upper range of the frequencies used in this study. The magnitude of the dispersion

($\Delta\varepsilon_{MWO}$) is estimated to be ~10. The frequency and dispersion magnitude is estimated assuming that surface conduction only takes place in the diffuse part of the double layer.

In the permittivity spectra measured for the polystyrene and core-shell particles used in this study only part of the MWO dispersion was observed at the highest measured frequencies (5-10 MHz). As the dispersion could not be measured due to the limited frequency range available, this dispersion type was not treated further. Furthermore, the above mentioned model has been developed for hard particles, and therefore would not apply for the core-shell particles.

4.2.2 α relaxation

Apart from the MWO relaxation described above, another relaxation process takes place at lower frequencies. Outside the particle double layer the anionic and cationic concentrations are the same, whereas inside the double layer the concentration of the counter-ion exceeds that of the co-ion. The field-induced flow of ions therefore results in a net reduction of the counter-ion concentration and an increase in co-ion concentration in the double layer which is in conflict with the electro-neutrality of the particle. To counteract this effect, a field-induced diffusion of ions around the double layer arises, which effectuates an increase of both the co- and counter-ion concentration on one side of the particle. This balances the flow of ions in and out of the double layer. As the flow of counter-ions opposes the field this results in an increase in the suspension permittivity. The balancing diffusion current does not occur instantly, but takes a time of approximately τ_α to establish due to the diffusion time around the particle double layer. The characteristic time of the α relaxation can be estimated as:

$$\tau_\alpha \approx \left(a + \kappa^{-1}\right)^2 / D \qquad \text{Eq. [13]}$$

For the size of the polystyrene particles and ionic concentrations used in this study this relaxation time is ~18 μs corresponding to a frequency of ~9 kHz which is far below the relaxation frequency of the MWO relaxation discussed in the previous section. Thus, the two relaxation processes should be well separated and easy to differentiate. The

magnitude of the α relaxation ($\Delta\varepsilon_\alpha$) has been found to be as high as approximately 1000 for polystyrene particles [45], which compared to $\Delta\varepsilon_{MWO}$ is several orders of magnitude higher.

4.2.3 Electrokinetic models

During the last century the theoretical understanding of the mechanisms behind dielectric dispersions of colloidal suspensions has gradually improved. The Maxwell-Wagner theory from 1914 was improved by O'Konski in 1960 to include the surface conductance of charged particles [66]. Schurr elaborated the O'Konski model by separating the surface conduction into a contribution from bound counter-ions and one from the diffuse part of the double layer [67]. In 1974 Dukhin and Shilov included the α relaxation into their model [68]. Until this point all the theoretical work was in the form of analytical expressions often including some approximation resulting in restrictions on either the electrokinetic potential, the value of κa or the ionic composition. The complexity of the set of equations needed to describe the dielectric dispersion and the approximation needed to obtain an analytical expression motivated DeLacey and White [69] to solve the electrokinetic equations numerically. They, however, omitted the acceleration term in the Navier-Stokes equation, restricting the model to frequencies below 10^5 Hz [70]. This limitation was later removed by Mangelsdorf and White [70]. In 1992 Kijlstra *et al*. [71] extended the theory of Fixman [72] to include a contribution to surface conductivity from the ions in the Stern layer. More recent, Hill *et al*. [73,74] and López-García *et al*. [75] have modelled the dielectric dispersion of particles with a polymeric shell. The model of hard sphere suspensions has also been further improved by using a cell model to allow modelling of the dielectric dispersion of suspensions with high particle volume fraction [76,77]. This model, however, does not include surface conduction.

Although the theoretical work is extensive, the agreement between modelled and measured dielectric dispersions is often found to be poor [47,78-84]. It seems that only when including the Stern layer conduction into the model a reasonable agreement is observed [84-86]. However, the introduction of Stern layer conduction also results in the

need of at least one extra parameter to describe the equilibrium between ions in the Stern layer and in the diffuse part of the double layer. This makes this type of model more difficult to use as information of this equilibrium may not always readily available. In this study it is found that both models with and without Stern layer conduction are unable to describe the measured dielectric dispersion. However, the inclusion of Stern layer conduction did improve the agreement between model and measurement in terms of the magnitude of the dispersion.

The inability of existing models to describe the observed dielectric dispersion in this study using realistic suspension parameters renders them inappropriate for describing the changes in dielectric spectra caused by flocculation. Furthermore, the models were developed for monodisperse, spherical, hard particles while their validity for non-spherical, porous aggregates with a broad distribution of sizes is questionable. For these reasons the use of physically based models are abandoned in this study, and instead an empirical expression is used for the description of the measured dielectric spectra. This will be further discussed in section 4.4.4.

4.3 Polymer characterisation by dielectric spectroscopy

The introduction of an alternating electric field in a solution of polyelectrolytes results in two distinct relaxation processes. In contrast to the relaxation of colloidal particles, the relaxation processes of polyelectrolytes have not received as much attention and the underlying mechanisms of the processes are not fully understood at this point. The available models are developed for solutions of polyelectrolytes containing counter-ion equivalents equal to the polyelectrolyte charge which is far from the case in the samples used in this study. The models can therefore not be used to quantitatively describe the measured permittivity spectra, but do offer some insight to the mechanisms responsible for the relaxation processes. As the processes are linked to the condensation of counter-ions to the polyelectrolyte, this area is treated briefly in section 4.3.1. The following sections 4.3.2 and 4.3.3 briefly describe the mechanisms that are believed to be the origin of the two relaxation processes.

4.3.1 Ion condensation on polyelectrolytes

In the two-state approximation where ions can either be condensed or free, condensation of counter-ions onto the polyelectrolyte takes place when the distance between polyelectrolyte charges (b) is smaller than the Bjerrum length (l_B) defined as:

$$l_B = \frac{e^2}{4\pi\varepsilon_0\varepsilon_m k_B T} \qquad \text{Eq. [14]}$$

The fraction of condensed ions (f_c) can be described by the Manning theory [87] and is calculated as:

$$f_c = \begin{cases} 1 - \dfrac{b}{l_B \left| z_p z_c \right|} & for\ b \le l_b \\ 0 & for\ b > l_b \end{cases} \qquad \text{Eq. [15]}$$

where z_p and z_c are the valences of the charges on the polyelectrolyte and of the counter-ions.

4.3.2 Relaxation of free counter-ions

When subjected to an electric field the free counter-ions (non condensed) polarise the polyelectrolyte perpendicular to the orientation of the backbone. The length scale of the polarisation process (L) at low ionic concentrations is of the order of polyelectrolyte separation distance and is therefore polymer concentration dependent. In a dilute solution, the time constant (τ_{free}) and the dispersion magnitude ($\Delta\varepsilon_{free}$) of the relaxation can be estimated as [88]:

$$\Delta\varepsilon_{free} \approx (1 - f_c) l_B \varepsilon_m N^{2/3} c_m^{1/3} \qquad \text{Eq. [16]}$$

$$\tau_{free} \approx \frac{L^2}{6D} \qquad \text{Eq. [17]}$$

Where N is the degree of polymerisation of the polyelectrolyte, c_m is the number concentration of polyelectrolyte monomers and D is the diffusion coefficient of the ions.
For the polymer concentration used in this study, a comparison with data for sulfonated polystyrene polymers [88] indicates that a relaxation of approximately 10^{-8} s could be

expected. This corresponds to a frequency of approximately 16 MHz, which is outside the measured frequency range used in this study. The permittivity spectra measured on the hydrophobically modified polymers show part of a relaxation process at frequencies between 1 and 10 MHz, but the full dispersion could not be measured due to the limitations on the measureable frequencies. Therefore, this relaxation process was not investigated in further detail.

4.3.3 Relaxation of condensed counter-ions

The condensed counter-ions polarise the polyelectrolyte when subjected to an electric field, but this polarisation takes places along the backbone rather than perpendicular to it, as was the case for the free counter-ions. Thus, the length scale of polarisation is in this case comparable to the characteristic size of the polyelectrolyte (R_p). The time constant (τ_{cond}) and the dispersion magnitude ($\Delta\varepsilon_{\mathrm{cond}}$) of the relaxation can be estimated as [88]:

$$\Delta\varepsilon_{\mathrm{cond}} \approx f_c l_{\mathrm{B}} \varepsilon_{\mathrm{m}} c_m R_p^{\,2} \qquad \text{Eq. [18]}$$

$$\tau_{\mathrm{cond}} \approx \frac{\gamma R_p^{\,2}}{6 k_{\mathrm{B}} T} \qquad \text{Eq. [19]}$$

where γ is the friction coefficient for the movement of the condensed counter-ions.

Typical relaxation time for this process is of the order 10^{-5} s [88] corresponding to a frequency of approximately 16 kHz, which is within the measureable frequency range.

4.4 Measurement of the dielectric spectrum

The dielectric spectrum is obtained by measurements of the frequency dependent impedance of the sample. Impedance (Z^*) is the complex resistance to an alternating electric field and has a component which is in phase with the field (the real part, Z') and one that is out of phase (the imaginary part, Z''). The impedance is obtained by subjecting the sample to an alternating electric field and determining the magnitudes of the oscillating

potential and current curves and the phase angle (φ) between them. This is illustrated in Fig. 4 where a complex plane illustration of the complex impedance also can be seen.

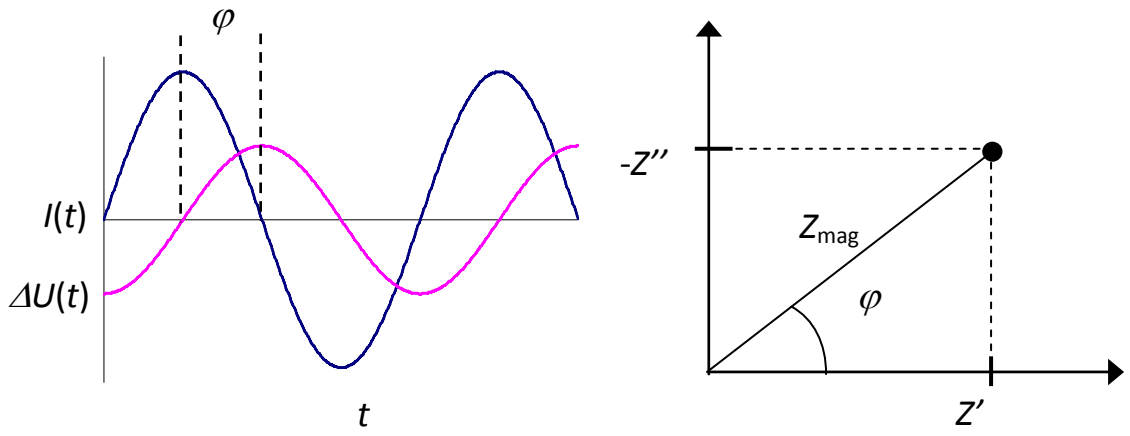

Fig. 4. Left: Time dependence of the alternating current and potential. The phase angle between the two curves is indicated. Right: Complex plane plot of the measured impedance.

The magnitude of the impedance is calculated as:

$$Z_{mag} = \frac{U_{mag}}{I_{mag}} \qquad \text{Eq. [20]}$$

For a pure conductor the impedance is independent of the frequency of the electric field, but when measuring the impedance of a suspension the dielectric properties of water and the colloids results in a change in impedance as a function of frequency. This is because of an increase in the relative importance of the dielectric properties when the frequency is increased. In this study a Solartron 1260 impedance analyser is used to measure the impedance of the samples. The resolution on the measured phase angle is 0.01 degrees. The apparatus is able to measure impedances in the range of 10 mΩ to 100MΩ in a frequency range of 10 μHz to 32 MHz. Only part of the available frequency range (1 kHz to 10 MHz) was used in the measurements as large errors were observed at frequencies outside this sub-range. The errors encountered at the highest frequencies are believed to originate from a lowering of the measurement quality near the upper frequency limit of the apparatus. The errors at low frequencies are discussed in detail in section 4.5.1.

4.4.1 Measurement cell

Measurement of the dielectric spectrum requires the use of measurement cell in which the sample is exposed to the alternating field the resulting impedance is measured. Such cells are traditionally constituted by a cylindrical spacer separating two parallel electrodes. This design is appealing due to its simple geometry. The specific design of such a cell is particularly important as several properties of the cell affect the quality of the measured impedance.

The cell material must be chosen carefully from its electrical properties. It is important that the conductivity of the material is as low as possible to prevent stray currents running outside the sample in the material of the cell. Likewise, the permittivity of the material must be low to reduce the stray capacitance of the cell. Most materials usable for the construction of the cell have very low conductivities but a significant, although low, dielectric constant. The result is that the cell material acts as a capacitor in parallel to the sample, thus contributing to the measured impedance. This cannot be completely avoided but still the choice of material is important to reduce the effect. In this study polysulphone was chosen as cell material due to its low conductivity ($<10^{-14}$ S/m) and dielectric constant (~3). Furthermore, polysulphone possess high mechanical strength, is resistant to acids and bases (pH 1-13) and maintains its properties over a wide temperature range (-100 to 150 °C).

In many cells used for colloidal characterisation the same set of electrodes is used to generate the field and to conduct the measurement. This setup has the disadvantage of including polarisation of the electrodes by dissolved ions into the measurement. The result is an extra contribution to the measured impedance from the polarisation of the electrodes. This contribution is often much larger than the contribution from the sample at low frequencies, but the effect diminishes as the frequency increases and is usually negligible at frequencies above 100 kHz [89]. Attempts have been made to solve this problem by using cells where variable electrode spacing is possible. As the dependence of the distance between the electrodes on the contributions from sample and electrode polarisation is different, measurements at variable electrode spacing has been used to identify and remove

the effect of the electrodes [90]. However, this method is somewhat cumbersome and time consuming. More recently a four-electrode cell has been developed in which one set of electrodes creates the electric field and another set placed in between conducts the potential measurement. As the polarisation of the electrodes only occurs if current passes through them, the use of a separate set of electrodes for the measurement almost removes the polarisation effects. This is due to the high impedance of the voltmeter circuit responsible for the potential measurement reducing the passing current to almost zero. As the four electrode design simplifies the measurement considerably and is more realistic for implementation in an industrial process, it has been chosen for the cell used in this study.

Two different types of electrode materials were chosen for the inner and outer electrode pairs. The outer field generating electrodes were made of glassy carbon disk and the inner measurement electrodes of platinum wire of 0.5 mm diameter. Platinum was chosen due to its excellent electrical properties resulting in a low degree of polarisation. As polarisation of the outer electrodes is of minor importance a cheaper solution was chosen for these electrodes.

In Fig. 5 the cell dimensions can be seen. Only one of the two half-cells is sketched in the figure. The cell constant is calculated as the ratio between the cross sectional area of the cylinder and the separation distance between the two platinum electrodes, and equates to 8.836 cm.

The outer electrodes are connected to the impedance analyser using coaxial cables, where simple copper wires are used to connect the platinum electrodes. The use of coaxial cables has the advantages of shielding against any influence from external electromagnetic waves, but also introduces a significant capacitance to the cable impedance. By using copper wire the parasitic capacitance is avoided, but is substituted by the problem of the influence of electromagnetic noise. This problem was addressed by spinning the two wires closely around each other thus forming a coil structure. Hereby any influence on by one of the wires is also experienced by the other. As the electrodes are used to measure the difference in potential between them any external influence is cancelled out as it affects the two wires equally.

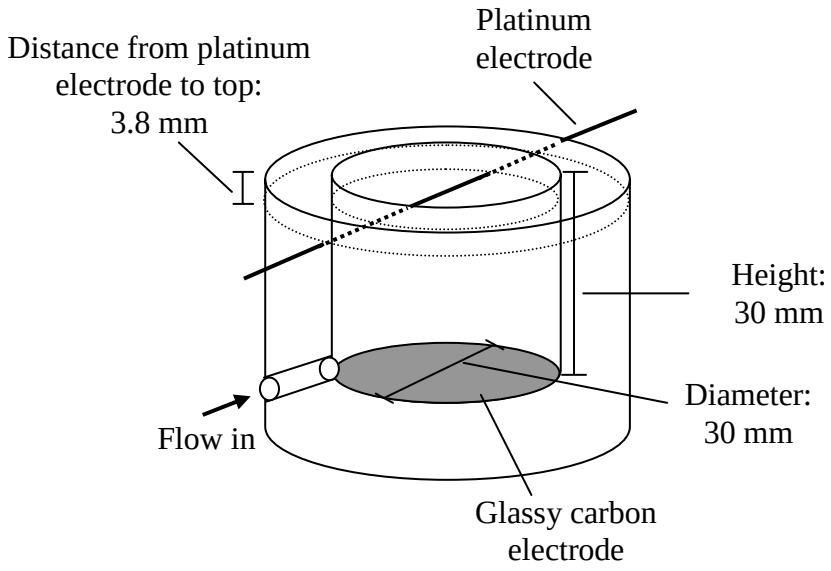

Fig. 5. Schematic drawing of one of the two half cells constituting the impedance measurement cell. In- and outlet for the suspension is placed in the ends near the glassy carbon electrodes. In the figure relevant dimensions are shown.

4.4.2 Correction for parasitic impedances

One of the problems involved in the measurement of sample impedance is the so-called parasitic impedances. These are unwanted contributions to the measured impedance arising from everything else than the sample, and can be caused by cables, stray capacitance, connections etc. Although care was taken to minimise the effects of such parasitic impedances during the design of the cell, measurements show that they are present in the measured impedance. In Fig. 6 the Bode plot of a 1 mM KCl solution is seen. Both the measured and the theoretical impedance are shown.

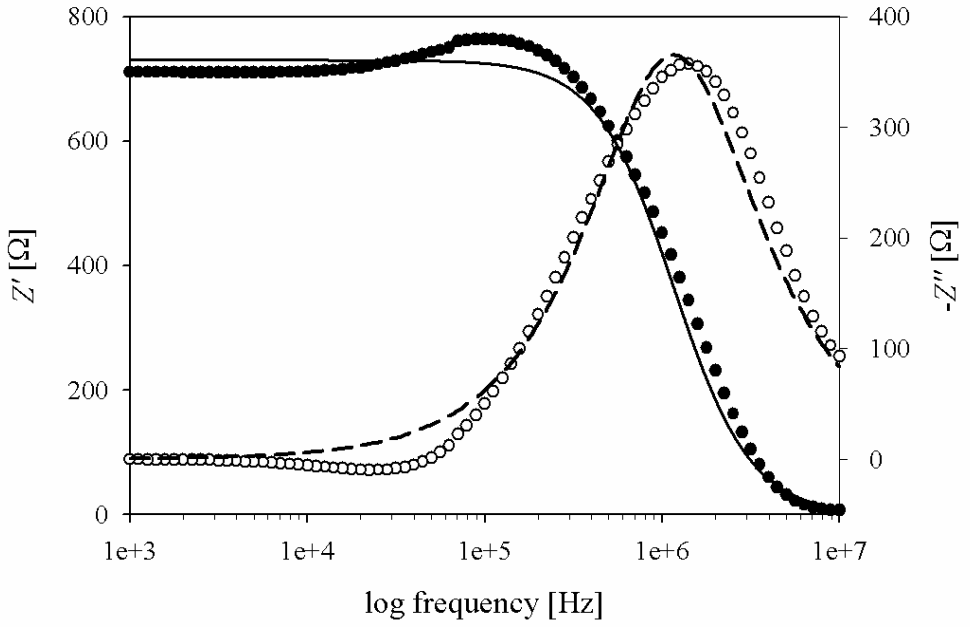

Fig. 6. Bode plot of a 1 mM KCl solution. (●) *Z'* and (○) *–Z''*. The lines show the calculated frequency dependence of the impedance.

It is evident that contributions apart from the sample are included in the measured spectrum. The presence of some parasitic impedances is unavoidable and in the literature different approaches have been used to handle this problem. In earlier studies equivalent electric circuits were used to model and remove the parasitic impedances. The concept of this approach is to identify the elements of to the parasitic impedance and chose appropriate electric components to represent them in an equivalent circuit model of the cell. An example of such a circuit model is shown in Fig. 7 [91]. Apart from the sample impedance the cell impedance is assumed to consist of a stray capacitance in parallel representing the capacitance of the cell and a serial impedance representing the cables.

Several such equivalent circuit models have been reported in the literature [91-94] and the number of included components in these references vary from 3 to 7. All of the proposed models have been used in an attempt to identify and remove the parasitic impedances

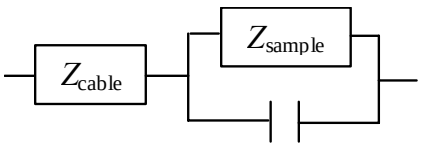

Fig. 7. Simple equivalent circuit model describing the measured impedance.

seen in Fig. 6, but none of them were capable of improving the measured impedance data satisfactory. A number of different modifications to the models found in the literature were made attempting to improve their description of the parasitic impedances but this was also unsuccessful. Thus the approach of using an equivalent circuit model was abandoned.

Another technique used for calibration is the short-open method. In this approach it is assumed that the parasitic impedances are comprised by a component in parallel to the cell and one component in series to this parallel circuit. These components can then be determined by conducting measurements of a short circuited cell (short measurement) and empty cell (open measurement). However this is fundamentally the same approach as the use of equivalent circuit models described above. The only difference is the short-open method determines the components by direct measurement, whereas they are identified by modelling when using the equivalent circuits. Thus, the use of this method was considered meaningless considering the lack of success using the equivalent circuit models.

Instead the short-open-load method was used to remove the unwanted impedances. In this technique the measurement cell is assumed connected to the impedance analyser through an electric quadrupole. The quadrupole is characterised by four frequency dependent coefficients that relates the input and output values of the current and voltage. These coefficients and determined by measurements of the short and open impedances (Z^*_{short} and Z^*_{open}) as discussed earlier, and a measurement of a so called load impedance ($Z^*_{\text{load,M}}$) which is a measurement with a sample of known impedance ($Z^*_{\text{load,R}}$) in the cell. From these three measurements the coefficients are determined, and it can be shown that the corrected value (Z^*_{c}) of a measured sample impedance (Z^*_{sample}) can be calculated as [91]:

$$Z^*_{\text{c}}(f) = \frac{Z^*_{\text{load,R}}(f)\left(1 - Z^*_{\text{load,M}}(f) \Big/ Z^*_{\text{open}}(f)\right)}{Z^*_{\text{load,M}}(f) - Z^*_{\text{short}}(f)} \frac{Z^*_{\text{sample}}(f) - Z^*_{\text{short}}(f)}{1 - Z^*_{\text{sample}}(f) Y^*_{\text{open}}(f)} \qquad \text{Eq. [21]}$$

Notice that all quantities in Eq. [21] are dependent on frequency, and so the short, open and load measurements must be carried out at the same frequencies used for the actual sample. Furthermore the impedance of the load sample must be similar to that of the

actual sample for the determination of the coefficients to be accurate. The gradual addition of flocculant to the sample in this study resulted in a gradual change in sample conductivity and for this reason several load measurements where made prior to each experiment. Aquatic solutions of potassium chloride at 30°C were used as load samples, and measurements of several hundreds of concentrations were made to insure that the difference between the load sample and the actual sample conductivity was small. The theoretical impedance of the load samples was determined from their conductivity (K_{load}) and relative permittivity (ε_{load}):

$$Z^*_{\text{load,R}}(f) = \frac{1}{k_{\text{cell}}\left(K_{load} + i2\pi f \varepsilon_0 \varepsilon_{load}\right)} \qquad \text{Eq. [22]}$$

The relative permittivity of the solutions is corrected for the presence of salt using an empirical expression proposed by Wang and Anderko [95]:

$$\varepsilon_{salt} = \frac{\varepsilon_{no\ salt}}{1 + \sum_i 0.519 X_i \ln\left(1 + 1.021 \cdot 10^6 \sqrt{I_X}\right)} \qquad \text{Eq. [23]}$$

Where X_i is the molar fraction of the ith ionic species and I_X is the ionic strength based on molar fractions. The changes in the dielectric constant were always less than 1%, and thus the validity of the empirical relationship is only of minor importance

Apart from parasitic impedances, electromagnetic waves originating from external sources may also influence the measured impedance. Such disturbances may originate from various electrical appliances and have a broad range of frequencies. To investigate the influence of any such electromagnetic disturbances an electrically grounded steel casing was build for the measurement cell. By placing the cell inside this casing it acts as a faraday cage and protects the measurement cell from electromagnetic waves. Several tests were conducted on solutions of KCl with and without the casing, but as no difference was observed it was removed from the setup due its inconvenience.

4.4.3 Calculating the permittivity from the measured impedance

In order to evaluate the dielectric properties of the sample the corrected impedance spectrum was converted to the equivalent values of conductivity and permittivity.

$$\frac{1}{Z^*} = G + i\omega C = k_{\text{cell}}\left(K + i\omega\varepsilon_0\left(\varepsilon' - i\varepsilon''\right)\right) = k_{\text{cell}}\left(K + \omega\varepsilon_0\varepsilon'' + i\omega\varepsilon_0\varepsilon'\right) \quad \text{Eq. [24]}$$

where G and C are the conductance and capacitance of the sample. The dielectric loss (which is a negative quantity) effectuates as a reduction in the apparent conductivity, and is therefore difficult to obtain without exact knowledge of the sample conductivity. For this reason only the real part of the complex permittivity is used.

To allow comparison of permittivity values measured as at different solid concentrations the measured permittivity is normalised by particle or polymer concentration (c) in kg/L:

$$\delta\varepsilon(\omega) = \frac{\varepsilon'(\omega) - \varepsilon_\infty}{c} \quad \text{Eq. [25]}$$

where ε_∞ is the high frequency value of the relative permittivity.

Ideally the particle volume fraction, rather than the concentration, should be used for the calculation of $\delta\varepsilon$. However, as the volume fraction is not well-defined in all the model systems of this study, concentrations have been used in all cases. The problem of defining the volume fraction arises when the particles are able to swell/de-swell due to changes in solution properties and/or adsorption of flocculants.

4.4.4 Modelling the dielectric spectrum

As discussed in section 4.2.3, the available physical models for a description of the dielectric dispersion are not suitable for use in this study. However, several empirical models of relaxation processes exist. Although not describing the relaxation in terms of physical properties of the colloidal suspensions, they provide the possibility of reducing the information in the measured dispersions to model parameters that can be used to describe the observed changes in the dielectric spectrum. The simplest of these are the Cole-Cole model [96], which describes the relaxation process in terms of its magnitude

($\Delta\varepsilon$), the relaxation time (τ), and the broadness of the dispersion represented by the parameter α.

$$\varepsilon^*(\omega) = \varepsilon_\infty + \frac{\Delta\varepsilon}{1+(i\omega\tau)^{1-\alpha}} \qquad \text{Eq. [26]}$$

where ε_∞ is the high frequency value of the permittivity.

In order to describe the normalised permittivity defined (Eq. [25]) instead of the complex permittivity, the model has been slightly altered by introducing a normalisation by particle or polymer concentration:

$$\delta\varepsilon(\omega) = \frac{\varepsilon'(\omega) - \varepsilon'_\infty}{c} = \mathrm{Re}\left(\frac{\Delta\varepsilon/c}{1+(i\omega\tau)^{1-\alpha}}\right) \qquad \text{Eq. [27]}$$

To ease the notation, the concentration normalised value of the modelled magnitude ($\Delta\varepsilon/c$) is denoted $\Delta\varepsilon_r$ from this point.

The model was fitted to the measured spectra by minimisation of a least square error function. Throughout the study it has been observed that the sensitivity of this error function to the α parameter was very low. This was further examined during the modelling of permittivity spectra of suspensions of polystyrene particles, where an analysis of parameter sensitivity was carried out. This analysis showed that the change in the error function resulting from a 10% change in either $\Delta\varepsilon$ or τ was approximately ten times higher than when making the same change in α. This shows that the modelled values of α cannot be considered as reliable as $\Delta\varepsilon$ and τ. Furthermore, for the particle suspensions the observed changes in α seemed to reflect the changes in τ. It could be argued that the particle aggregation causing changes in τ would also induce changes in α due a broadening in the distribution of time constants, but it may also be an effect of the low sensitivity of this parameter. For the hydrophobically modified polymers such correlation between τ and α was not observed as the α values decreased throughout the experiment. Whether the observed changes in α can in fact be related to flocculation process or are artefacts of the model fitting has not been determined, and thus this parameter has not been used to evaluate the flocculation process.

4.5 Evaluation of dielectric measurements

The measurement of the dielectric spectrum is a non-trivial task as several factors may influence the quality of the measurement. Furthermore, a number of factors that are not directly related to the flocculation process may potentially influence the dielectric spectrum. In this section the quality and sensitivity of the measurement is investigated to ensure that the observed changes in the dielectric dispersions can be related to the flocculation process.

4.5.1 Quality of corrected permittivity

To check the effect of the short-open-load calibration on the measured permittivity data a series of load measurement were carried out followed by a series of measurements on solutions of KCl of different concentrations. The resulting values of $\varepsilon(f)$ and $K(f)$ can be seen in Fig. 8 for solutions of 3, 5 and 10 mM KCl.

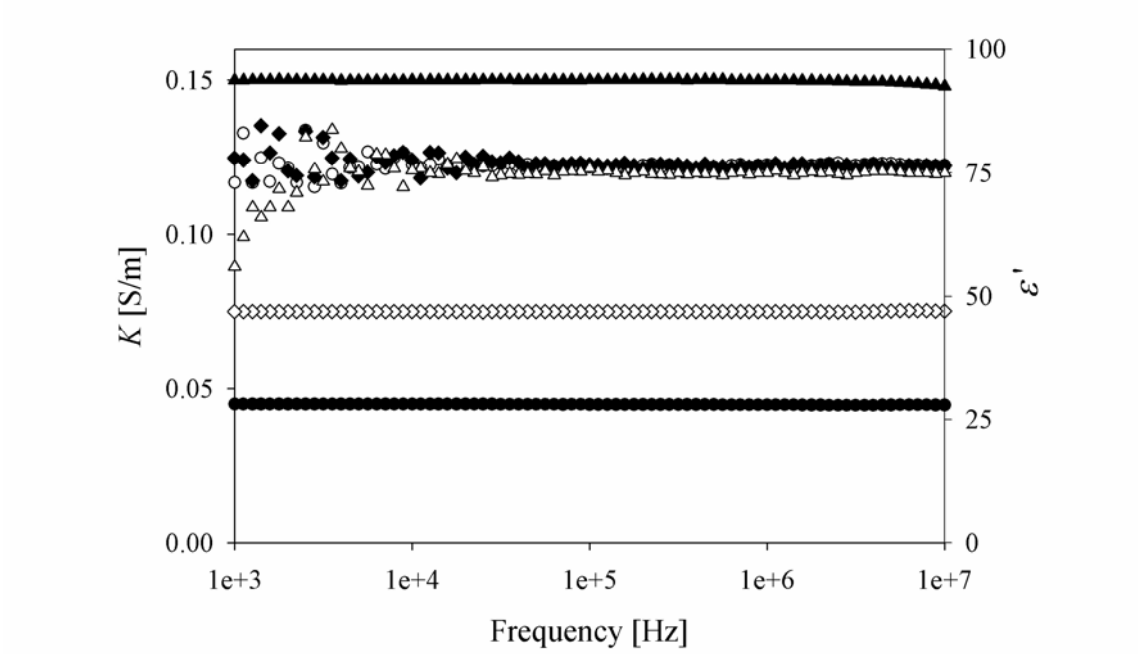

Fig. 8. Frequency dependence of the conductivity (K) and relative permittivity (ε') of KCl solutions. (●) K(3 mM), (○)ε'(3 mM), (◇) K(5 mM), (◆) ε'(5 mM), (▲) K(10 mM), (Δ) ε'(10 mM).

The conductivities of all three solutions are constant throughout the frequency range at values that match the theoretical conductivities. At high frequencies the relative permittivities are also constant all at the same value of approximately 76.5. This is very close to the permittivity of water at 30°C which is 76.6. The small difference is caused by the presence of KCl in the solution. However, at frequencies below ~10 kHz the relative permittivity starts to scatter with relative standard deviation of up to 5%. The scattering gets worse as the frequency is decreased. This is presumably caused by electrode effects that have not been sufficiently removed by the calibration process. Several attempts have been made to improve the quality of the calibration at low frequencies, but without success. Such attempts include increase of integration time during the measurement, shortening of cables and change of distance between platinum electrodes. Although the scattering is significant for the observed solutions of KCl, the relative importance is small when measuring suspensions of low frequency permittivities several orders of magnitude higher than that of water. Therefore, the calibration procedure is found to be acceptable for measurements within the frequency range of 1 kHz to 10 MHz.

For the 10 mM KCl solution the relative permittivity is seen to systematically decrease at frequencies below approximately 3 kHz. This is an effect of the limitations on phase angle resolution of the apparatus. As the conductivity of the sample increases the phase angle (φ) measured at a given frequency (f) is reduced. When the value of the phase angle becomes comparable to the resolution of the apparatus, the quality of the measured data must be expected to decrease drastically. By equating the phase angle with the resolution, the critical frequency where this problem theoretically occurs can be estimated as [92]:

$$f = \tan(\varphi)\frac{K(f)}{2\pi\varepsilon_0\varepsilon(f)} \qquad \text{Eq. [28]}$$

Using a conductivity of 0.15 S/m results in a frequency of approximately 6 kHz. Comparing this value with observed value of 3 kHz, indicates that the estimation of critical frequency is a worst case scenario, and that slightly higher frequency can be measured.

4.5.2 Reproducibility of permittivity spectrum

The reproducibility of the DS measurement has been tested on several levels. Repeated measurements on solutions of KCl have been carried out and in all cases the resulting spectra are similar to the data in Fig. 8. Furthermore, the dielectric spectrum of polystyrene particle suspensions have been measured several times independent of each other. In Fig. 9 such measurements can be seen and the variations between the spectra are found to be small.

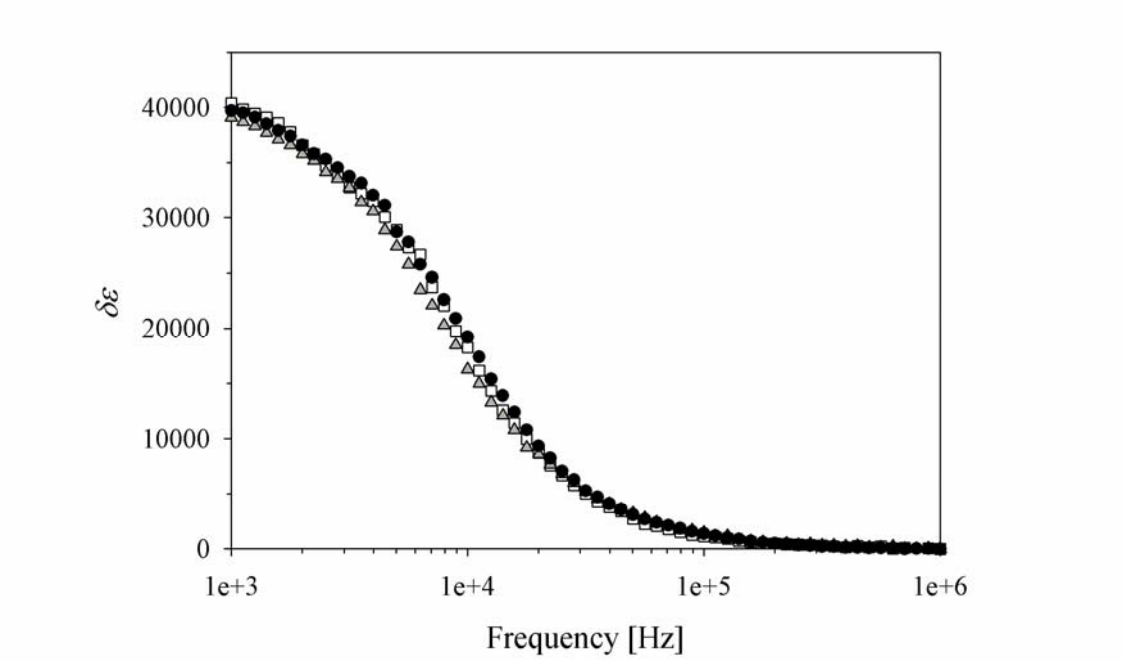

Fig. 9. Frequency dependence of $\delta\varepsilon$ for three different measurements of the same polystyrene particle suspension.

Finally, the reproducibility of the spectra obtained during a flocculation experiment has been tested by conducting an experiment twice under the same conditions. Two suspensions of polystyrene particles (ϕ = 2.6%) were flocculated using poly(DADMAC) polymer, and the resulting dependence of the permittivity spectrum on the polymer dosage investigated. Each spectrum was reduced to the three parameters of the Cole-Cole model,

and in Fig. 10 $\Delta\varepsilon_r$ and τ can be seen as a function of polymer dosage for the two experiments. The α parameter is not shown for reasons discussed in section 4.4.4.

The overall reproducibility of the measurement is found to be good, and the variations in model parameters obtained from similar suspensions are small compared to the variations observed during the flocculation process.

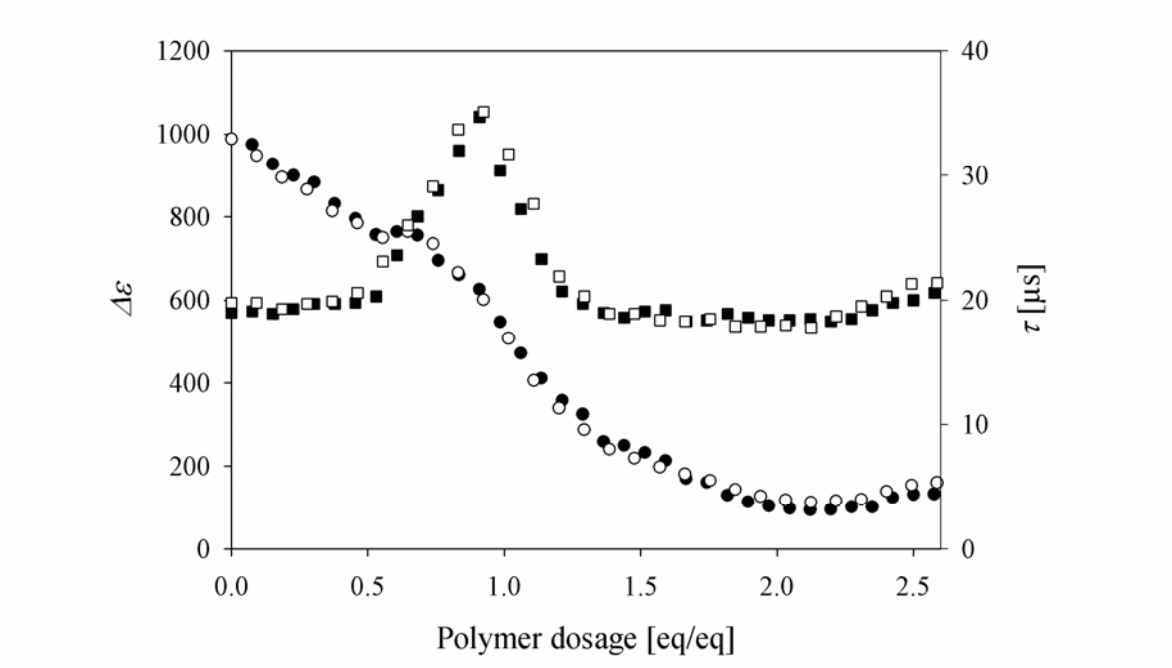

Fig. 10. The model parameters $\Delta\varepsilon$ (circles) and τ (squares) as a function of polymer dosage for two independent flocculation experiments (black and white symbols).

4.5.3 Effect of flowing sample

In the experimental setup the sample is pumped through the cell during measurement. To investigate whether the flow of the sample had any influence on the permittivity spectrum, measurements with and without flow were made on the same suspension of polystyrene particles. As the differences were small and comparable to what was found in Fig. 9, it was concluded that the flowing suspension did not influence the measurement noticeable.

4.5.4 Effect of un-adsorbed polymers

When flocculating colloidal particles with cationic polymers, the adsorption of polymer to the particle surface is believed to be strong and the presence of un-adsorbed polymers in the bulk phase should therefore be limited. Thus, no influence of dissolved polymers on the measured permittivity spectrum is expected. However, as un-adsorbed polymers give rise to a dielectric dispersion themselves, their presence may potentially influence the measured permittivity making it difficult to relate observed changes to the flocculation process. Therefore the potential influence of un-adsorbed polymer has been investigated to ensure that their presence does not significantly influence the permittivity spectrum of the colloids. In Fig. 11 the frequency dependent permittivity can be seen for concentrations of polyDADMAC of 30, 60, and 300 mg/L. The lowest concentration corresponds to the concentration needed to induce flocculation of a polystyrene particle suspension (ϕ = 2.6%).

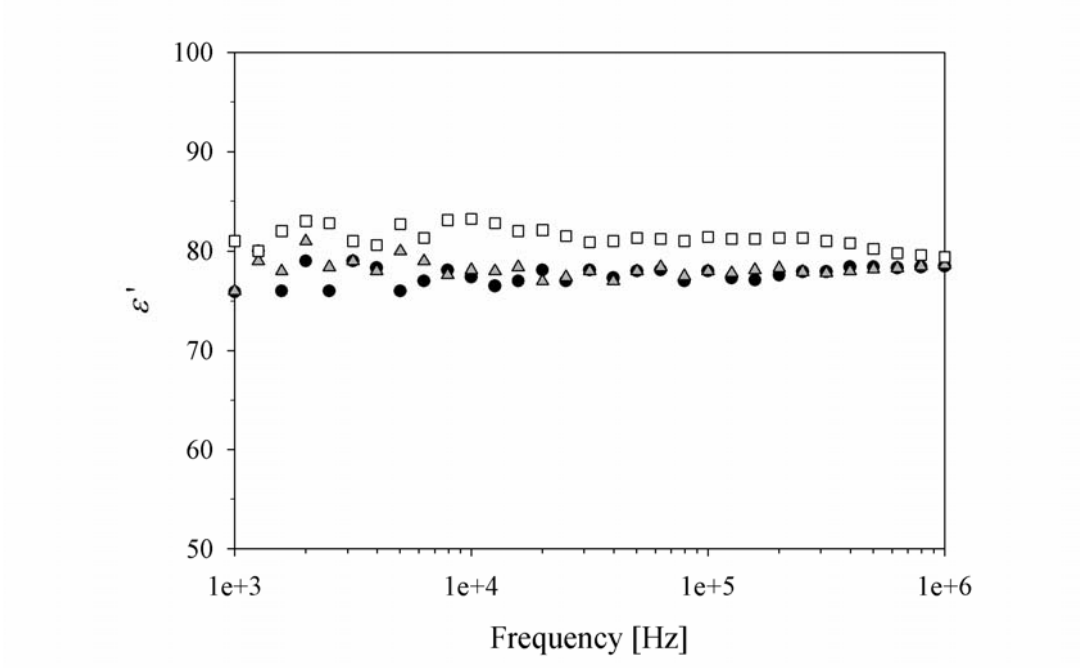

Fig. 11. Permittivity of three poly(DADMAC) solution as a function of frequency. (●) 30 mg/L, (△) 60 mg/L, (□) 300 mg/L.

No influence of the added polymer is seen at the level of dosages used in the flocculation experiments of polystyrene particle, but at higher concentrations a small increase in the permittivity is seen down to 10 kHz. However, the presence of un-adsorbed polymers in that concentration is unlikely even in the flocculation experiments of the core-shell particles where the polymer demand is higher. Thus, it can be concluded that the influence of un-adsorbed polymer is negligible.

4.5.5 Effect of ionic strength on relaxation of polystyrene particles

The addition of polymelectrolytic flocculant during a flocculation experiment increases the conductivity of the suspension partly due to the polymer counter-ions and partly due to the release of adsorbed ions from the particle surface. As the dielectric dispersion of colloidal suspensions is dependent on the ionic concentrations in the suspension [78], the effect of the ionic strength on the permittivity spectrum was investigated. In Fig. 12 the permittivity spectra of a polystyrene particle suspensions with different concentrations of KCl are seen.

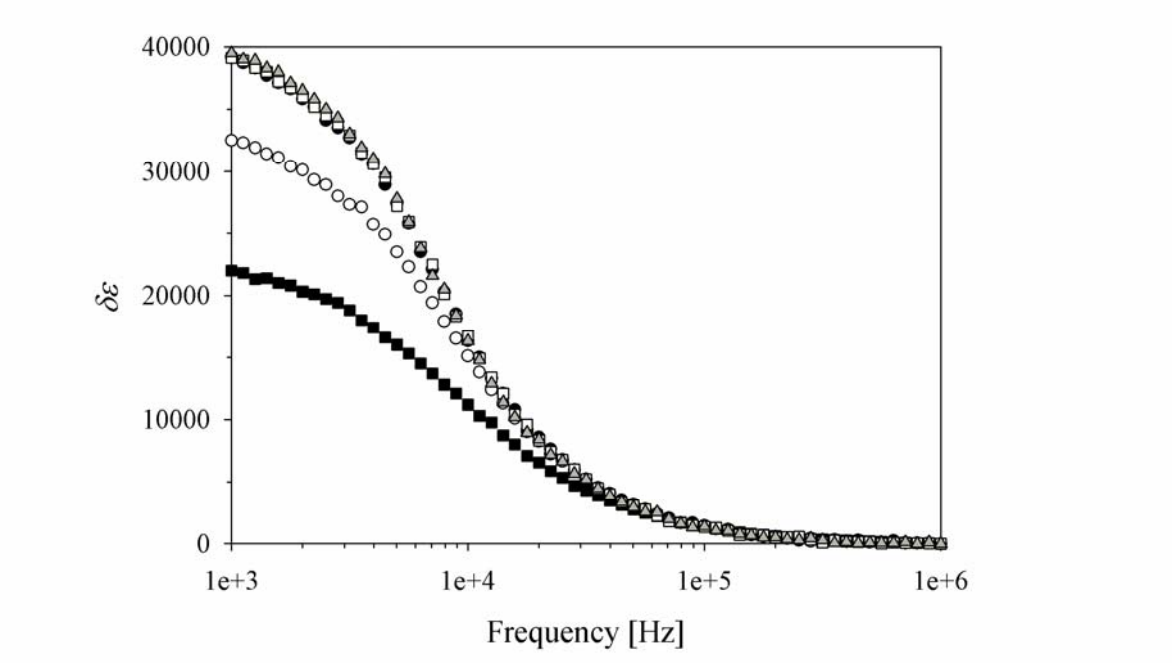

Fig. 12. Effect of KCl concentration on the frequency dependence of $\delta\varepsilon$ for a suspension of polystyrene particles. (■) 1 mM, (○) 2 mM, (●) 3 mM, (□) 4 mM, (△) 10 mM.

The magnitude of the dispersion increases up to 3 mM, and is then unaffected by further increment in the concentration. Although a more thorough investigation of the dependence of the dispersion in the concentration range of 0-3 mM is of interest from an electrokinetic point of view, it is not within the scope of this study.

From the data in Fig. 12 it is evident that a background electrolyte concentration of 3 mM KCl diminishes the influence of further addition of ions. As the estimated changes in ionic concentrations caused by the addition of polymer throughout the whole flocculation and deflocculation process of the polystyrene particles are less than 1 mM, the final concentration is well within the concentration range investigated in Fig. 12. Thereby it is ensured that observed changes in the dielectric spectrum are caused by the polymer-particle interaction and not by a change in conductivity.

5. Flocculation of model systems

The effect of flocculation on the dielectric dispersion was studied using the setup described in section 3.2. The measured dielectric spectra was analysed and modelled as described in section 4.4. This procedure yields the magnitude and the relaxation time of the dielectric dispersion as a function of the polymer dosages added to a suspension. In the following chapter the observed changes in the dielectric dispersion as a result of the flocculation process are presented.

5.1 Impact of flocculation on relaxation time

5.1.1 Hydrophobically modified polymers

In Fig. 13a and b two examples of how the relaxation time of the polymer solutions changes as function of barium dosage is seen for the HMPAA-0 and the HMPAA-8 polymers. The barium dosage is given as equivalent barium charges per equivalent polymer charges. The figures also show the $RATIO_R$ signals measured with the PDA.

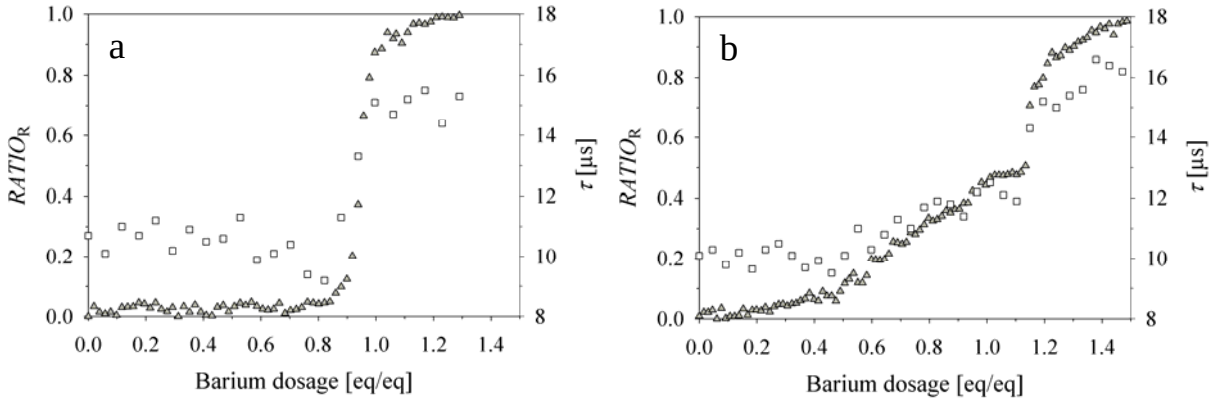

Fig. 13. $RATIO_R$ (△) and τ (□) as a function of barium dosage for the flocculation of hydrophobically modified poly(acrylic-acid). a) HMPAA-0 and b) HMPAA-8.

For the HMPAA-0 polymer the $RATIO_R$ signal is constant at dosages below 0.8 eq/eq indicating that no change in the stability of the polymers takes place. At a dosage of approximately 0.9 eq/eq a steep increase is observed indicating the formation of polymer aggregates.

For the HMPAA-8 the $RATIO_R$ signal is also constant at low dosages, but only up to 0.2 eq/eq where it begins to increase slightly. This increase continues up to a dosage of approximately 1.1 eq/eq where a steep increase, similar to that found for the HMPAA-0, is observed. The occurrence of the 'shoulder' in the $RATIO_R$ signal is interpreted as the result of the hydrophobic chains making the polymers less soluble, thereby initiating aggregation at lower barium dosages. However, complete aggregation is not observed until a dosage similar to that observed for the HMPAA-0 is reached, thereby signifying the importance of charge neutralisation for complete destabilisation.

For both the HMPAA-0 and the HMPAA-8 the relaxation time is seen follow the same tendencies as the $RATIO_R$ signal; a steep increase in τ is found where the $RATIO_R$ signal increases steeply and a 'shoulder' in τ is observed for the HMPAA-8. As τ is related to a characteristic length of polymers or aggregates hereof, it is expected to increase upon the formation of aggregates, which is also the case. The results obtained for the hydrophobically modified polymer are discussed in greater detail in paper 4.

Some variations in the modelled values of τ are observed when looking at Fig. 13a and b. These fluctuations are caused by a reduced data quality which results from 1) the low dispersion magnitude of the polymer relaxation process rendering the influence of measurement noise relatively more important and 2) the high ionic strength that follows from the adjustment of pH to 9.3 that increases the lower limit of the measureable frequency (see section 4.5.1).

The agreement between the observed changes in the relaxation times and $RATIO_R$ signal as exemplified in Fig. 13a and b were found for all five degrees of hydrophobic modification. The relaxation time can therefore be used to monitor the formation of aggregates from the hydrophobically modified polymers.

5.1.2 Core-shell particles

Fig. 14 shows the changes in the relaxation time of the 11%AA core-shell particle suspension as a function of polymer dosage (LMW). The polymer dosage is given as polymer charge equivalents per particle charge equivalents. In the figure the $RATIO_R$ signal from the PDA is also seen. The $RATIO_R$ signal is constant at dosages up to 0.4 eq/eq where it increases and reaches a maximum at 0.55 eq/eq. This is caused by a flocculation of the particles. It is seen that this maximum corresponds well with the point of zero mobility. Further increasing the dose causes the $RATIO_R$ signal to decrease due to a deflocculation of the aggregates. This is caused by an overdosing of the polymer resulting in charge reversal.

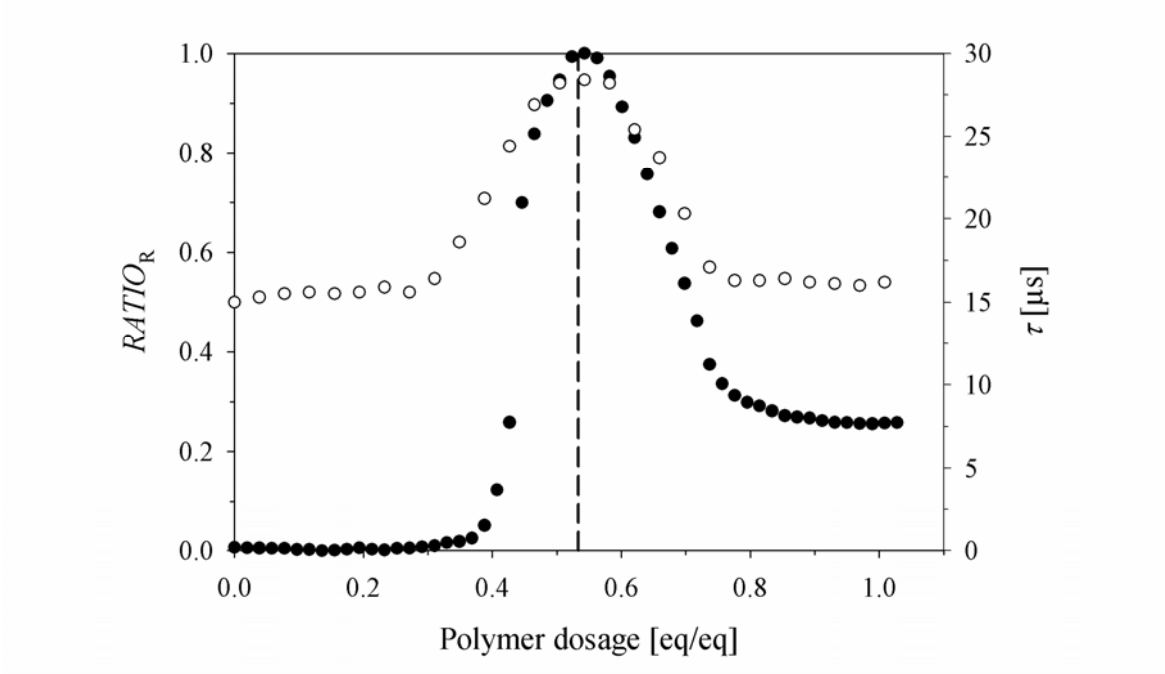

Fig. 14. $RATIO_R$ (●) and τ (○) as a function of polymer dosage for the flocculation of 11%AA core-shell particles. The vertical punctured line shows polymer dosage required to reach zero electrophoretic mobility

The relaxation time shows similar behaviour as the $RATIO_R$ signal, as a peak is found at the same polymer dosage. This agreement was found for both the used polymer types (LMW and HMW), and also for particles with thicker acrylic acid shells. However, for the

37%AA and the 54%AA particles the complete process of flocculation and deflocculation, as observed in Fig. 14, could not be followed by neither DS nor PDA, as the interaction between the flocculation polymer and the acrylic acid polymer chains on the particles resulted in the formation sticky particle surfaces. This caused a complete removal of particles and aggregates from the suspension as they adhered to almost any surface in the experimental setup. This phenomenon, which made further measurements impossible, took place before the flocculation peak was reached, but after the $RATIO_R$ signal and τ start to increase. Up to this point, though, the agreement between the $RATIO_R$ signal and the relaxation time was good. The results obtained from the experiments with the core-shell particles, are discussed in further detail in paper 3.

The experiments showed that the relaxation time increased when particle flocculation occurred and decreased again when deflocculation was introduced. This shows its usability as an indicator of the state of flocculation for core-shell particles.

5.1.3 Polystyrene particles

In Fig. 15a-c the relaxation time is seen as a function of polymer dosage for suspensions of polystyrene particles flocculated using a) poly(DADMAC), b) Zetag 7633 and c) Zetag 7867FS40. The polymer dosages are given as polymeric charge equivalents per particle charge equivalents. The residual turbidity is also seen in the figures. For polymer types the addition of polymer results in a reduction of the residual turbidity, which is an effect of particle flocculation. For the poly(DADMAC) polymer the residual turbidity increases again when a dosage of approximately 2 eq/eq is reached indicating the onset of deflocculation. No deflocculation is observed for the Zetag 7867FS40 polymer as the residual turbidity remains very close to zero even at very large polymer dosages. For the Zetag 7633 polymer a peak is observed at approximately 1.25 eq/eq, which is interpreted as a rearrangement of the floc structure.

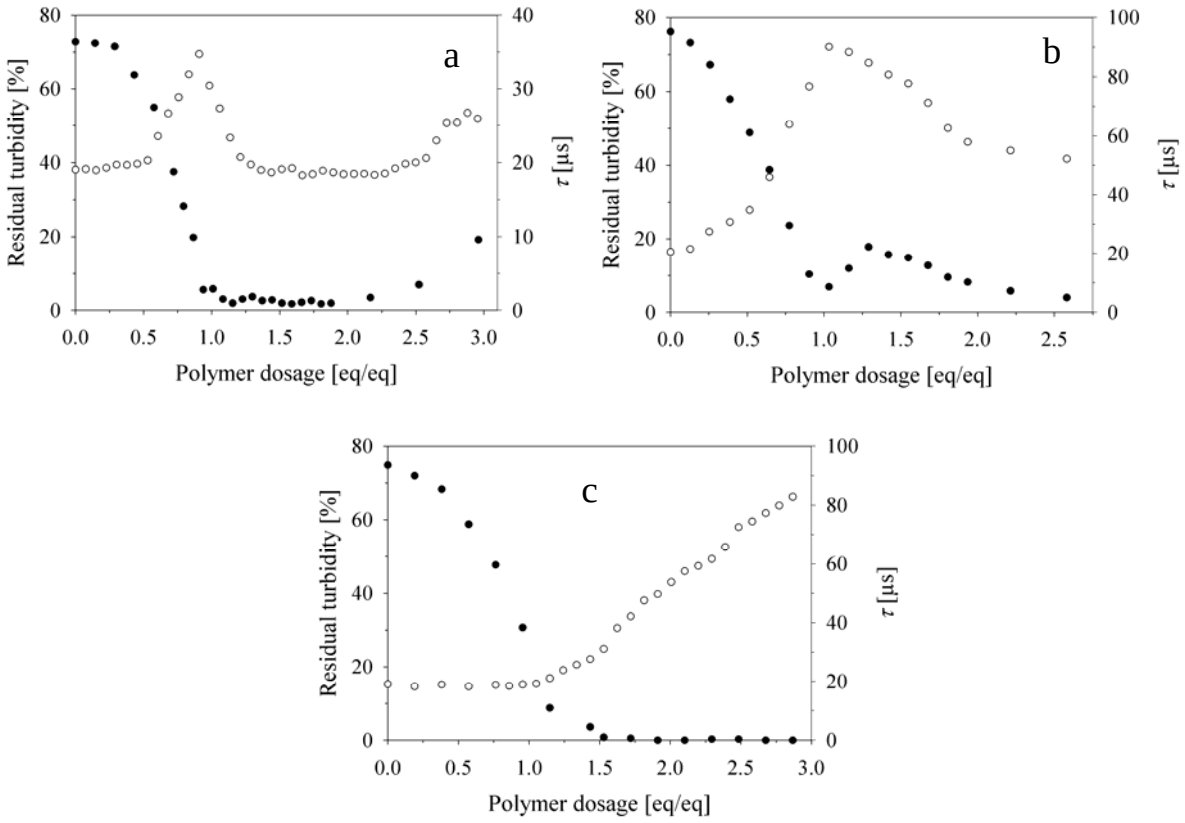

Fig. 15. Residual turbidity (●) and τ (○) as a function of polymer dosage for the flocculation of polystyrene particles. a) poly(DADMAC), b) Zetag 7633, c) Zetag 7867FS40.

The relaxation times are found to increase as polymer is added for all three polymer types, and the increases seem to agree with the onset of the flocculation process. For the poly(DADMAC) polymer the relaxation time begins to decrease again at a polymer dosage of 0.9 eq/eq, whereas deflocculation is not observed before reaching a dosage of 2 eq/eq. Such disagreement between the residual turbidity and the relaxation time does not seem to be present for the Zetag 7867FS40 polymer where the continued increase in τ agrees with the zero value of the residual turbidity. For the Zetag 7633 polymer a decrease in τ is observed at the same dosage where the residual turbidity begins to increase, and for this reason it is interpreted as an effect of the same structural rearrangements of the aggregates. These results are more thoroughly discussed in paper 1 and 2.

The relaxation time is observed to increase when the particle aggregates start forming, however its usability for evaluating the continued flocculation process of the polystyrene particles is not unambiguous. It seems that the type of flocculant, and thereby the resulting floc structure, is important in determining the applicability of τ for the evaluation of the process. When using the poly(DADMAC) polymer it is clear that τ is not an ideal parameter for evaluating the whole flocculation process, whereas its use seems more appropriate for the two Zetag polymers.

5.1.4 Summary

As mentioned in sections 4.2.2 and 4.3.3 the relaxation time of a single spherical particle or polymer molecule can be estimated from the characteristic diffusion distance. In the particle case the characteristic distance is equal to $a+\kappa^{-1}$ (Eq. [13]). For the suspensions of polystyrene particles, with the lowest ionic strength used in this study, $a\kappa = 34$ and so $a \gg \kappa^{-1}$. Thus for simplicity, it is reasonable to assume the diffusion distance equal to *a*. For the polymers an estimate of the characteristic length is the radius of gyration. When aggregation occurs, a larger, porous structure is formed. This results in an increase in the diffusion distance. If the floc is considered a particle itself the size can be estimated from the relaxation time using Eq. [13]. It is, however, unlikely that this equation will provide reasonable estimations of the floc size as the flocs not necessarily are spherical and their porosity allows ionic flow inside the structure. Furthermore, the fractal structure often found in flocs may result in the polarisation of substructures inside the floc rather than of the floc itself. This will result in relaxation times that are considerable smaller than what would be expected from the floc size using Eq. [13]. Finally, the ionic environment inside the floc may be different than in the bulk, so that the diffusion coefficients of ions may be smaller inside the floc. This also renders any quantitative use of Eq. [13] difficult. Thus, this equation cannot be used to assess the floc size from the relaxation time. Presently, no theoretical expressions relating the relaxation time of flocculated structures to their size exist. This makes any quantitative determination of the floc size from the dielectric dispersion impossible. However, the relaxation can be used

qualitatively to assess changes in the floc size as seen in previous sections, but it should be kept in mind that the floc structure as well as the size is expected to influence the observed relaxation times.

The lower value of the frequency range used in this in this study (1 kHz) limits the relaxation times that can be observed. Using

$$\tau = \frac{1}{\omega} = \frac{1}{2\pi f} \qquad \text{Eq. [29]}$$

a limit of τ < 160 µs is found to correspond to a frequency of 1 kHz. Thus, if floc-structures with relaxation times above this limit are formed their contribution to the dispersion is not seen in the measured dielectric spectrum. Assuming that Eq. [13] is applicable for these structures the resulting size is ~ 1.1 µm. Although the value of this limit is believed to be erroneous, due to the lack of applicability of Eq. [13] to the aggregate structures in question, it still serves to show that only the dielectric dispersion caused by fairly small flocs and particles can be expected to be observed in the spectrum. As the flocs formed during flocculation almost always are much larger than this limit (10 µm being a small aggregate), the relaxation time of some of the aggregates will become too large to be observed and thereby disappear from the measured dispersion. This results in a decrease in the observed relaxation time due to the removal of high value contributions from the large flocs to the average value of τ found from the model fitting. The extent of this decrease depends on the fraction of flocs that are removed from the measured spectrum and the size of the remaining flocs and particles. It is this phenomenon that is believed to be the reason for the poor agreement between τ and the flocculation which is observed during the flocculation of polystyrene particles with poly(DADMAC).

If the formed aggregates are porous with a low fractal dimension it is possible that substructures of the aggregate are polarised. In this case it is the size of such substructures, rather than the size of the aggregate itself, that determines the relaxation time. Therefore very large aggregates may still contribute to the measured dielectric dispersion as long as the polarised substructures of the aggregate do not have relaxation times above the above mentioned limit. The effect of contributions from large aggregates moving out of the measured frequency window is thus a larger problem for dense flocs than for flocs with an

open structure. This may explain the improved agreement between τ and the flocculation process which is observed when using the Zetag polymers, rather than poly(DADMAC), to flocculate the polystyrene particles.

For the core-shell particles the presence of the partly swollen shell makes the formation of polarisation over small length scales possible although the particles are incorporated into an aggregate. This seems to prevent the problem with time constants moving out of the frequency window. However, it cannot be ruled out that relaxation processes related to the whole aggregate occur which have large relation times that are found at frequencies below the lover limit of measurement.

In the case of the polymer aggregates the problem with part of the dispersion moving out of the frequency window does not seem to exist either. The explanation may be that the formed aggregates are fairly small as compared to the particle aggregates found for polystyrene and core-shell particles. Furthermore, as the polymer aggregates have porous structures, polarisation processes may take place inside the aggregates resulting in the observed relaxation times.

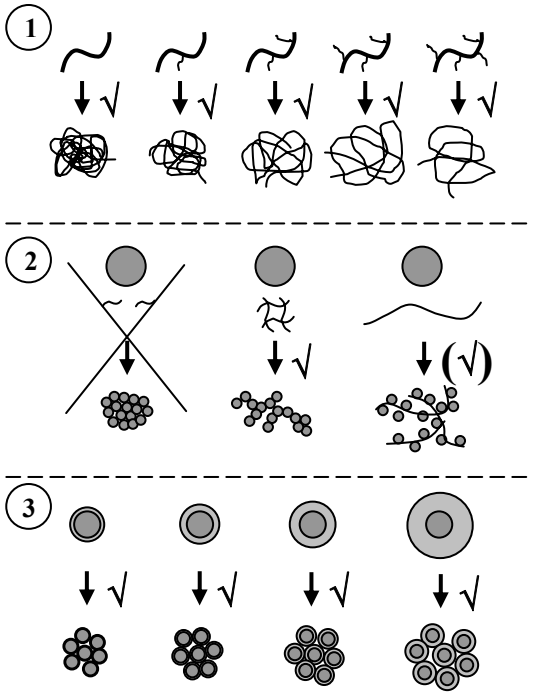

Fig. 16. Schematic overview of the ability of DS to monitor the flocculation processes by use of the relaxation time as an aggregation indicator. √, (√) and X shows whether the use of DS was successful, partly successful or without success.

When summarising the results of using τ to evaluate the flocculation processes, it is useful to keep in mind Fig. 2 in which the model systems and their expected aggregate structures were sketched. In Fig. 16 this figure has been slightly modified to show the experiments were the use of τ to evaluate the flocculation process was found applicable. Although the rate of success observed for the polystyrene particles is low, the suspension/

solution type does not solely determine whether τ can be used or not. The structure of the resulting aggregate seems to be a controlling factor as well, as the formation of dense flocs causes problems.

5.2 Impact of flocculation on dispersion magnitude

5.2.1 Hydrophobically modified polymers

Fig. 17 shows the magnitude of the dielectric dispersion ($\Delta\varepsilon_r$) as a function of barium dosage for the flocculation experiment of the HMPAA-0 polymer solution. The $RATIO_R$ signal, which has been described in section 5.1.1, is also seen. The addition of barium results in a small decrease in $\Delta\varepsilon_r$ until a dosage of approximately 0.9 eq/eq is reached. Here $\Delta\varepsilon_r$ increases markedly and then becomes almost constant. The increase agrees well with the onset of aggregation. Similar behaviour is observed for the all polymer types, and these results are discussed in further detail in paper 4. Thus, for the hydrophobically modified polymers it seems that the dispersion magnitude is influenced by the aggregation process.

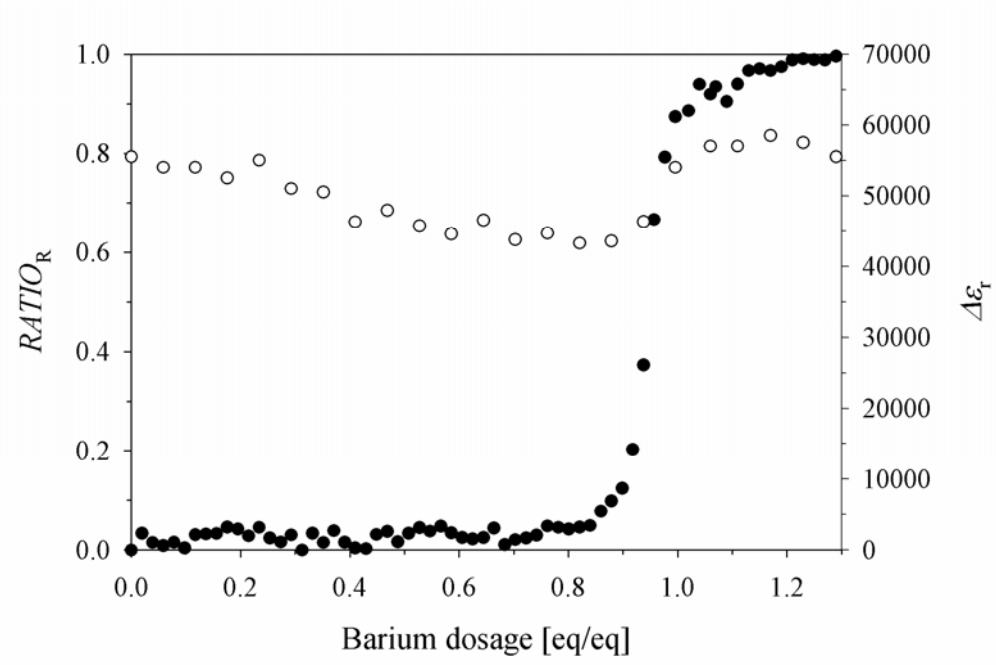

Fig. 17. $RATIO_R$ (●) and $\Delta\varepsilon_r$ (○) as a function of barium dosage for the flocculation of hydrophobically modified poly(acrylic-acid).

5.2.2 Core-shell particles

In Fig. 18 $\Delta\varepsilon_r$ is seen as a function of LMW polymer dosage for the 11%AA particle suspension. The $RATIO_R$ signal, which described in section 5.1.2, is also shown. Furthermore, the dosage required to reach zero electrophoretic mobility is shown as a vertical line. The dispersion magnitude decreases markedly as the polymer is added. At a polymer dosage of 0.38 eq/eq a minimum is reached and $\Delta\varepsilon_r$ starts to increase. This point is seen to correspond to the onset of flocculation rather than the point of zero mobility. Similar behaviour is found for all the core-shell particles, and these results are discussed in further detail in paper 3. It therefore seems that the dispersion magnitude is influenced by the aggregation process of the core shell particles, as was also the case for the hydrophobically modified polymers.

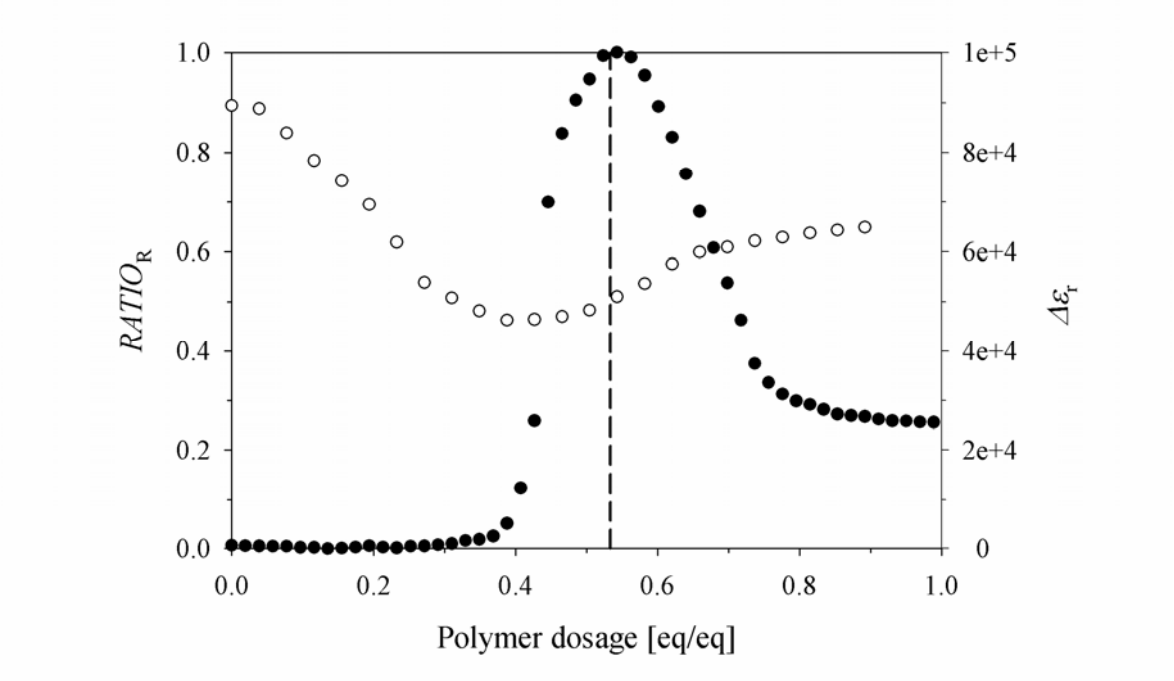

Fig. 18. $RATIO_R$ (●) and $\Delta\varepsilon_r$ (○) as a function of polymer dosage for the flocculation of 11%AA core-shell particles.

5.2.3 Polystyrene particles

Fig. 19a-c show $\Delta\varepsilon_r$ as a function of polymer dosage for the flocculation of polystyrene using a) poly(DADMAC), b) Zetag 7633 and c) Zetag 7867FS40. Furthermore, the residual turbidity, described in section 5.1.3, is shown, and the point of zero electrophoretic mobility is indicated by a vertical line. A detailed description of the results is given in paper 1 and 2.

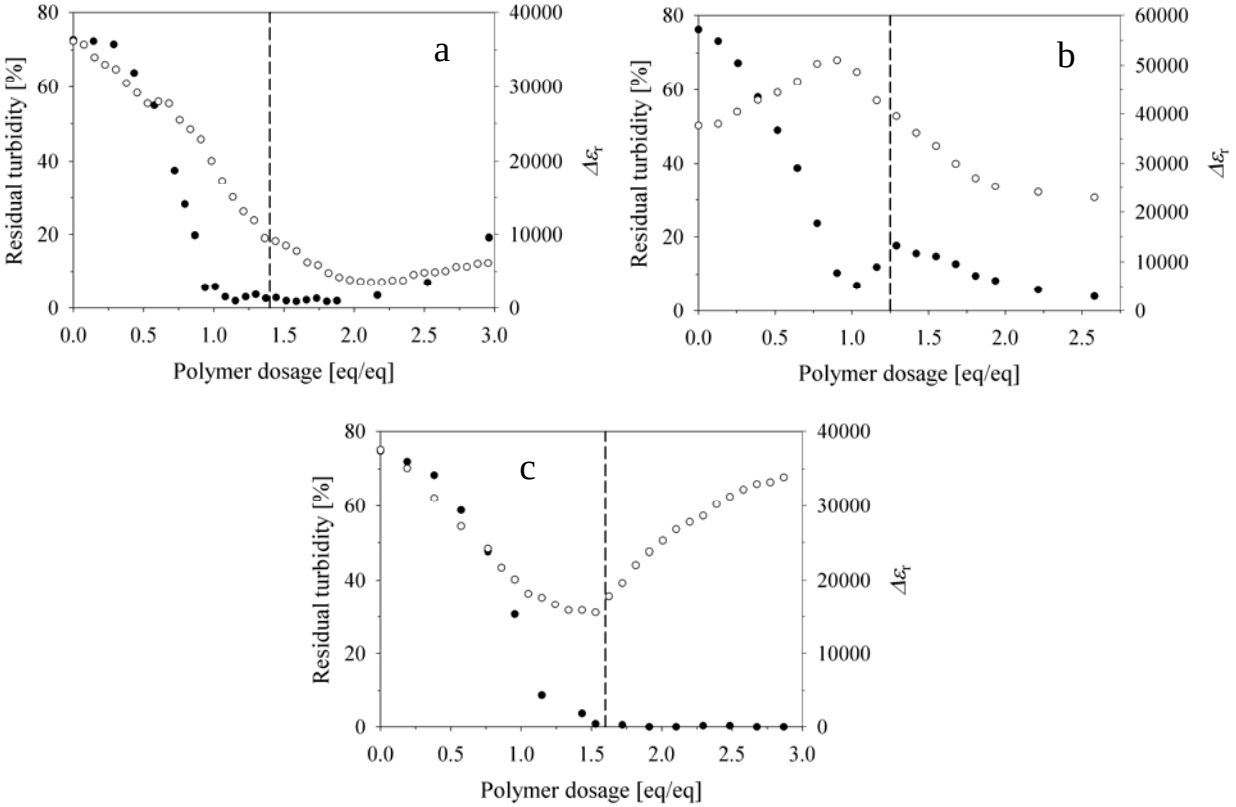

Fig. 19. *RATIO*$_R$ (●) and $\Delta\varepsilon_r$ (○) as a function of polymer dosage for the flocculation of polystyrene particles. a) poly(DADMAC), b) Zetag 7633, c) Zetag 7867FS40.

For poly(DADMAC) the addition of polymer initially decreases the dispersion magnitude. Apart from a small peak, which is found at the onset of flocculation where the residual turbidity is low, the decrease continues up to a dosage of approximately 2.25 eq/eq. From this point a slight increase is observed. No correlation between the point of zero mobility and the changes in $\Delta\varepsilon_r$ seems to present.

The addition of Zetag 7867FS40 polymer also decreases the magnitude initially. The slope of this decrease is reduced when reaching a dosage of approximately 1 eq/eq where flocculation also starts to take place. At a dosage of 1.5 eq/eq, which corresponds to the point of zero mobility, $\Delta\varepsilon_r$ begins to increase.

For Zetag 7633 an initial increase in $\Delta\varepsilon_r$ is observed when adding the polymer. When the residual turbidity reaches the minimum, $\Delta\varepsilon_r$ begins to decrease. This decrease levels of at higher dosages and does not seem to be influenced by the point of zero mobility.

5.2.4 Summary

The dielectric dispersions observed for the polymer solutions originate from the diffusion of condensed counter-ions along the polymer backbone. Adding barium to the solutions causes the formation of chelates between the barium ions and the charged groups on polymer. The effect of these complexes on the dispersion magnitude has never been investigated, and thus their influence is unknown. Considering the complex-bound barium ions as condensed ions, the formation of complexes is expected to increase the dispersion magnitude due the higher fraction of condensed ions (f_c). However, the formation of barium-polymer complexes releases some of the initially condensed ions, as they are no longer needed once the polymer charge is reduced by the chelates. Furthermore, the reduction of polymer charge reduces the radius of gyration, and thereby the characteristic length scale of the polymer, due a larger degree of coiling. This acts to reduce the dispersion magnitude, as seen in Eq. [18]. From the experiments it is evident that the magnitude decreases due to the addition of barium, indicating a reduction of the radius of gyration. At higher dosages, the formation of aggregates increases the characteristic length scale and thus results in an increase in $\Delta\varepsilon_r$.

The origin of the α relaxation found for suspensions of colloidal particles is the particle charge, as this is what causes the formation of the electric double layer. Thus, the magnitude of the dispersion due to the α relaxation is strongly dependent on the particle charge and will disappear if the particle charge is neutralised. Inverting the sign of the charge causes the dispersion to reappear. The size of the induced dipole due to polarisation

also affects the magnitude of the dispersion. Experimental results [45] and theoretical studies [69,76,97] of single particle suspensions show that the magnitude increases with particle size, and in some studies slight aggregation has been proposed as an explanation of unexpected high values of the magnitude [86,98].

Thus, the effect of adding cationic polymers to the anionic particles will affect the magnitude of dispersion in two opposing directions. While the neutralisation of particle charges causes a decrease in the magnitude, the growth in aggregate size acts to increase it. The relative influence of the two contributions depends on the extent of charge reduction required to facilitate flocculation and the size of the formed flocs (or substructures of the flocs).

For the core-shell particles the initial observed decrease in $\Delta\varepsilon_r$ is interpreted as the reduction of particle charge. At the onset of flocculation, the influence of size on $\Delta\varepsilon_r$ begins to dominate and it increases. Similar behaviour is observed for the polystyrene particles flocculated with the Zetag 7867FS40 polymer, but here the reversal of particle charge as well as aggregation seems to be responsible for the increase in $\Delta\varepsilon_r$. For the polystyrene particle flocculated with the Zetag 7633 polymer, where bridging is believed to occur, the effect of aggregation on $\Delta\varepsilon_r$ dominates even at low dosages, as the charge reduction of this polymer is ineffective due to the formation of loops and tails. This results in the observed increase in $\Delta\varepsilon_r$.

The disappearance of dispersion contributions originating from structures with large relaxation times, as described in section 5.1, also affects the magnitude of the dispersion. As the magnitude is determined by the number of polarised structures, as well as their degree of polarisation, the removal of such structures from the measurement results in a decrease in the magnitude of the observed dispersion. For the polystyrene flocculated with poly(DADMAC) it is this effect that causes the continued decrease of $\Delta\varepsilon_r$ even after aggregation has started.

Generally, the dispersion magnitude is found to increase when aggregation occurs, but the concurrent influence of the charges on the magnitude clouds the influence of the aggregation processes. Thus, the use of the dispersion magnitude to evaluate the flocculation process does not seem to be as effective as the relaxation time. However, the

potential of this parameter to evaluate the remaining particle charges in a suspension still makes it useful, although more research is needed.

6. The use of DS as a flocculation monitor

In the previous chapter the influence of the flocculation process on the parameters obtained by DS was investigated. It was found that the relaxation time in certain cases is a usable parameter for evaluating the extent of flocculation, and that the structure of the formed aggregates seems to determine the applicability. As the relaxation time related to the overall length scale of the aggregates is often too high to be found inside the measureable frequency range, it is necessary that the aggregates contain polarisable substructures with lower relaxation times. The presence of such substructures is more likely to be found in aggregates with an open structure. Thus, the use of DS to monitor flocculation process requires that the formed aggregates have a non-compact structure.

The quality of the measured dielectric dispersion was found to be influenced by the suspension conductivity and the solids concentration. High conductivities (say >0.2 S/m) reduced the capability of measuring at low frequencies, thereby removing important information from the dielectric spectrum. This problem, however, can partly be overcome by using an apparatus of higher phase angle resolution. Furthermore, low solids concentrations resulted in small dispersion magnitudes, and thus poor signal-to-noise ratios. Therefore, optimal results are obtained for suspensions of high solids concentration and low conductivity.

The use of DS for evaluation of flocculation processes is not without problems. Both suspension and aggregate characteristics must satisfy certain criteria to ensure the applicability of the measurement. Restrictions on the suspension characteristics are, however, a general limitation of all available methods used for evaluation of flocculation, and therefore not a specific disadvantage found for DS. An example hereof is the limitation to dilute suspensions found for most available techniques. The opposite is found to be the case for DS, which works best at high solid concentrations, thereby further underlining its area of applicability.

When the use of DS in ‘real’ suspensions is to be tested, the above considerations need to be taken into account, and the suspension and flocculation type must be chosen on

the basis of these. The process of flocculating sewage sludge to improve dewatering is expected to meet these criteria, as the solid concentration is fairly high (5-10 g/L), the conductivity is low (approximately 0.1 S/m [99]) and the sludge flocs have an open, water swollen structure [100].

The discussion of the use of DS has so far been limited to flocculation processes. However, the technique also has the potential to monitor the stabilisation, rather than destabilisation, of suspensions. If the purpose of chemical dosing is to prevent aggregation then the desired product (the stable suspension) is likely to have relaxation times within the measureable frequency range, why DS may be used to monitor the process. Examples of such processes are found in the production of paints and yoghurt, where high stability is needed.

Generally, processes in which structural components are formed can potentially be monitored using DS. Such processes could be the formation of biofilm on a surface or the formation of a fouling layer on a separation membrane. By monitoring the formation of structures with a relaxation time that differs from the relaxation time of its bulk constituents such processes may be evaluated.

When implementing DS to a ‘real’ application it is important to choose a design that minimises the influence of parasitic impedances. This preferably means platinum electrodes, a four electrode setup, a simple measurement geometry and short cables from the measurement cell to the impedance analyser. For practical reasons this may not always be achievable, and thus the measurement quality may be reduced on this account.

The measurement time is also an important issue when discussing the implementation of DS to a ‘real’ application. Theoretically a frequency scan in range from 1 kHz to 1 MHz can be carried out in less than a second, but as the measurement quality greatly improves by measuring over a large number of field oscillations, in practice it may take minutes. Naturally, the measurement time also depends on the number of different frequencies included in the scan. Thus, it is a trade-off between measurement quality and/or data point resolution on one side and measurement time on the other. If the requirements for the time resolution of the measurement are high, a lower data quality may be the price.

7. Conclusion

The use of dielectric spectroscopy for the evaluation of flocculation processes was investigated in this study. An experimental procedure for evaluating the method was developed and tested to ensure that observed changes in the dielectric spectrum could be attributed to the flocculation process. Using model compounds, flocculation processes involving a variety of suspension and aggregate properties were studied, and the use of dielectric spectroscopy to monitor the processes were evaluated.

Generally, it was found that relaxation time obtained from the measurement of dielectric spectroscopy was a usable parameter for monitoring the process, as it increased upon formation of aggregates. However, formation of densely packed aggregate seemed to cause problems, rendering the use of dielectric spectroscopy inappropriate.

The magnitude of the dielectric dispersion was also observed to be influenced by the aggregation process as it increased when flocculation was introduced. Furthermore, the magnitude could be related to the reduction of particle charge in the flocculation processes of particle suspension. As the influence of both aggregation and charge on this parameter makes it more difficult to interpret, it is considered less applicable for an evaluation of the flocculation process as compared to the relaxation time.

List of symbols and abbreviations

Roman letters

a	Particle radius [m]
c	Particle or polymer concentration [kg/L]
c_m	Number concentration of polyelectrolyte monomer [m^{-3}]
C	Capacitance [F]
D	Diffusion coefficient [m^2/s]
DC	Voltage equivalent to the average value of the transmitted light [V]
e	Elementary charge [C]
E_0	Electric field in the vacuum [V/m]
E_m	Electric field in the medium [V/m]
f	Frequency [Hz]
f_c	Fraction of condensed ions [-]
G	Conductance [S]
i_m	Current density in the medium [A/m^2]
i_p	Current density in particle [A/m^2]
I_{mag}	Magnitude of the oscillating electrical current [A]
I_X	Ionic strength based on molar fractions
k_B	Boltzmann constant [J/K]
k_{cell}	Cell constant [m]
K	Conductivity [S/m]
K_{load}	Conductivity of load sample [S/m]
K_m	Conductivity of medium [S/m]
K_p	Conductivity of particle [S/m]
K^σ	Surface conductivity of particle [S]
K^σ_d	Surface conductivity of the diffuse part of the double layer [S]
K^σ_i	Surface conductivity of the inner part of the double layer [S]
l_B	Bjerrum length [m]
L	Polarisation length [m]

N	Degree of polymerisation [-]
R_p	Characteristic size of polyelectrolyte [m]
$RATIO$	Ratio between RMS and DC [-]
$RATIO_{\max}$	Maximum value of $RATIO$
$RATIO_{\min}$	Minimum value of $RATIO$
$RATIO_{\mathrm{R}}$	Normalised value of $RATIO$
RMS	Root mean square value of the difference between DC and the transmitted light [-]
t	Turbidity [-]
t_R	Relative turbidity function [-]
T	Temperature [K]
U_{mag}	Magnitude of the oscillating electrical potential [V]
X	Molar fraction
z	Ion valency [-]
z_c	Valency of condensed ion [-]
z_p	Valency of polyelectrolyte charge [-]
Z^*	Complex impedance [Ω]
Z'	Real part of the complex impedance [Ω]
Z''	Imaginary part of the complex impedance [Ω]
Z^*_{c}	Corrected complex impedance [Ω]
$Z^*_{\mathrm{load,R}}$	Theoretical complex impedance of sample [Ω]
Z^*_{open}	Complex impedance of empty cell [Ω]
Z_{mag}	Magnitude of the complex impedance [Ω]
Z^*_{sample}	Measured complex impedance of sample [Ω]
Z^*_{short}	Complex impedance of short circuited cell [Ω]

Greek letters

α	Parameter describing the broadness of the dielectric dispersion [-]
$\delta\varepsilon$	Permittivity increment [L/kg]
$\Delta\varepsilon$	Magnitude of dielectric dispersion [-]
$\Delta\varepsilon_{cond}$	Magnitude of the dispersion caused by polarisation of condensed counter-ions [-]
$\Delta\varepsilon_{free}$	Magnitude of the dispersion caused by polarisation of free counter-ions [-]
$\Delta\varepsilon_{MW}$	Magnitude of the MW dispersion [-]
$\Delta\varepsilon_{MWO}$	Magnitude of the MWO dispersion [-]
$\Delta\varepsilon_r$	Normalised magnitude of dielectric dispersion [-]
ε^*	Complex relative permittivity [-]
ε'	Real part of the complex relative permittivity [-]
ε''	Imaginary part of the complex relative permittivity [-]
ε_0	Permittivity of vacuum [F/m]
ε_∞	Relative permittivity at high frequency [-]
ε_{load}	Relative permittivity of load sample [-]
ε_m	Relative permittivity of medium [-]
$\varepsilon_{no\ salt}$	Relative permittivity of sample without the presence of salt [-]
ε_p	Relative permittivity of particle [-]
ε_{salt}	Relative permittivity of sample in the presence of salt [-]
ϕ	Particle volume fraction [-]
γ	Friction coefficient [N s/m]
η	Viscosity [Pa s]
φ	Impedance phase angle [rad]
κ	Inverse Debye length [m^{-1}]
λ	Wavelength [m]
θ	Parameter describing the ratio between surface conductivity from the inner and diffuse parts of the double layer [-]

τ	Relaxation time [s]
τ_{α}	Relaxation time of the α relaxation process [s]
τ_{cond}	Relaxation time of condensed counter-ions [s]
τ_{free}	Relaxation time of free counter-ions [s]
τ_{MW}	Relaxation time of the MW dispersion [s]
ω	Angular frequency [rad/s]
ζ	Zeta potential [V]

Abbreviations

DADMAC	Diallyldimethylammoniumchloride
DS	Dielectric spectroscopy
HMPAA	Hydrophobically modified poly(acrylic-acid)
HMW	High molecular weight
LMW	Low molecular weight
MW	Maxwell-Wagner
MWO	Maxwell-Wagner-O'Konski
PDA	Photometric dispersion analyser
PSA	Particle size analyser
SCD	Streaming current detector

References

[1] X. Yu, P. Somasundaran, J. Colloid Interface Sci. 177 (1996) 283.

[2] M. Hjorth, M. L. Christensen, P. V. Christensen, Bioresour Technol 99 (2008) 8598.

[3] H. Saveyn, S. Meersseman, O. Thas, P. Van der Meeren, Colloids and Surfaces a-Physicochemical and Engineering Aspects 262 (2005) 40.

[4] A. Ayol, S. K. Dentel, A. Filibeli, Water Sci Technol 50 (2004) 9.

[5] J. Gregory, Critical Reviews in Environmental Control 19 (1989) 185.

[6] E. Dickinson, L. Eriksson, Adv. Colloid Interface Sci. 34 (1991) 1.

[7] J. Gregory, J. Colloid Interface Sci. 42 (1973) 448.

[8] K. Aoki, Y. Adachi, J. Colloid Interface Sci. 300 (2006) 69.

[9] D. H. Bache, Water Sci Technol 50 (2004) 55.

[10] D. H. Bache, C. Johnson, J. F. McGilligan, E. Rasool, Water Sci Technol 36 (1997) 49.

[11] F. Bouyer, A. Robben, W. L. Yu, M. Borkovec, Langmuir 17 (2001) 5225.

[12] P. Borget, F. Lafuma, U. Bonnet-Gonnet, J. Colloid Interface Sci. 284 (2005) 560.

[13] S. Biggs, M. Habgood, G. J. Jameson, Y.-d. Yan, Chem Eng J 80 (2000) 13.

[14] M. Elimelech, C. R. O'Melia, Langmuir 6 (1990) 1153.

[15] L. Eriksson, B. Alm, P. Stenius, Colloids and Surfaces a-Physicochemical and Engineering Aspects 70 (1993) 47.

[16] A. Fan, N. J. Turro, P. Somasundaran, Colloids and Surfaces A: Physicochemical and Engineering Aspects 162 (2000) 141.

[17] A. S. Moussa, M. Soos, J. Sefcik, M. Morbidelli, Langmuir 23 (2007) 1664.

[18] S. Neyret, L. Ouali, F. Candau, E. Pefferkorn, J. Colloid Interface Sci. 176 (1995) 86.

[19] O. Oulanti, J. Widmaier, E. Pefferkorn, S. Champ, H. Auweter, J. Colloid Interface Sci. 294 (2006) 95.

[20] R. Podgornik, M. Licer, Curr. Opin. Colloid Interface Sci. 11 (2006) 273.

[21] X. Yu, P. Somasundaran, J. Colloid Interface Sci. 178 (1996) 770.

[22] A. Vaccaro, J. Sefcik, H. Wu, M. Morbidelli, J. Bobet, C. Fringant, AIChE J. 52 (2006) 2742.

[23] S. S. Shenoy, R. Sadowsky, J. L. Mangum, L. H. Hanus, N. J. Wagner, J. Colloid Interface Sci. 268 (2003) 380.
[24] J. Gregory, D. W. Nelson, A New optical method for flocculation monitoring, Solid-Liquid Separation, Ellis Horwood, Chichester, 1984.
[25] G. Li, J. Gregory, Water Res 25 (1991) 1137.
[26] P. V. Christensen, K. Keiding, J. Colloid Interface Sci. In Press
[27] W. F. Gerdes, 12th National ISA Analysis Instrument Symp., Houston, Texas, (1966)
[28] S. K. Dentel, K. M. Kingery, Water Sci Technol 21 (1989) 443.
[29] S. K. Dentel, K. M. Kingery, Journal American Water Works Association 81 (1989) 85.
[30] S. K. Dentel, A. V. Thomas, K. M. Kingery, Water Res 23 (1989) 413.
[31] S. K. Dentel, A. V. Thomas, K. M. Kingery, Water Res 23 (1989) 423.
[32] P. H. Cardwell, J. Colloid Interface Sci. 22 (1966) 430.
[33] C. A. Walker, J. T. Kirby, S. K. Dentel, J. Colloid Interface Sci. 182 (1996) 71.
[34] R. J. Hunter, Foundations of Colloid Science, Oxford University Press, New York, 2001.
[35] G. C. Jeffrey, R. H. Ottewill, Colloid & Polymer Science 266 (1988) 173.
[36] S. Tang, C. M. McFarlane, G. C. Paul, C. R. Thomas, Colloid Polym. Sci. 277 (1999) 325.
[37] L. Wågberg, J. Eriksson, Chem Eng J 80 (2000) 51.
[38] J. Kilander, S. Blomstrom, A. Rasmuson, Chem. Eng. Sci. 61 (2006) 7651.
[39] P. Mpofu, J. Addai-Mensah, J. Ralston, Int. J. Miner. Process. 71 (2003) 247.
[40] A. McFarlane, K. Bremmell, J. Addai-Mensah, Miner. Eng. 18 (2005) 1173.
[41] M. S. Nasser, A. E. James, Colloids and Surfaces a-Physicochemical and Engineering Aspects 301 (2007) 311.
[42] B. H. Chen, S. J. Lee, D. J. Lee, L. Spinosa, Drying Technology 24 (2006) 1289.
[43] H. W. Campbell, P. J. Crescuolo, Water Sci Technol 14 (1982) 475.
[44] M. M. Abu-Orf, S. K. Dentel, Journal of Environmental Engineering-Asce 125 (1999) 1133.
[45] H. P. Schwan, G. Schwarz, J. Maczuk, H. Pauly, J. Phys. Chem. 66 (1962) 2626.

[46] F. Mantegazza, T. Bellini, V. Degiorgio, A. V. Delgado, F. J. Arroyo, J. Chem. Phys. 109 (1998) 6905.
[47] R. Barchini, D. A. Saville, J. Colloid Interface Sci. 173 (1995) 86.
[48] M. Balastre, J. Persello, A. Foissy, J. F. Argillier, J. Colloid Interface Sci. 219 (1999) 155.
[49] I. Pochard, P. Couchot, A. Foissy, Colloid Polym. Sci. 276 (1998) 1088.
[50] J. Gregory, J. Colloid Interface Sci. 55 (1976) 35.
[51] M. L. Jimenez, F. J. Arroyo, J. van Turnhout, A. V. Delgado, J. Colloid Interface Sci. 249 (2002) 327.
[52] K. Asami, J. Non-Cryst. Solids 305 (2002) 268.
[53] S. Krairak, K. Yamamura, M. Nakajima, H. Shimizu, S. Shioya, J Biotechnol 69 (1999) 115.
[54] C. M. Harris, R. W. Todd, S. J. Bungard, R. W. Lovitt, J. G. Morris, D. B. Kell, Enzyme Microb Technol 9 (1987) 181.
[55] B. Boudakian, R. M. Hill, T. A. Strivens, L. A. Dissado, Colloid Polym. Sci. 269 (1991) 938.
[56] F. Bordi, C. Cametti, J. S. Tan, D. C. Boris, W. E. Krause, N. Plucktaveesak, R. H. Colby, Macromolecules 35 (2002) 7031.
[57] M. Mandel, Biophys Chem 85 (2000) 125.
[58] G. H. Markx, D. B. Kell, Biofouling 2 (1990) 221.
[59] A. Pribush, H. J. Meiselman, D. Meyerstein, N. Meyerstein, Biorheology 37 (2000) 429.
[60] W. Kuang, S. O. Nelson, J. Colloid Interface Sci. 193 (1997) 242.
[61] J. C. Maxwell, A treatise on Electricity and Magnetism, Clarendon Press, Oxford, 1873.
[62] K. W. Wagner, Archiv für Elektrotechnik 2 (1914) 371.
[63] K. W. Wagner, Archiv für Elektrotechnik 3 (1914) 100.
[64] G. Blum, H. Maier, F. Sauer, H. P. Schwan, J. Phys. Chem. 99 (1995) 780.
[65] J. J. Bikerman, Zeitschrift Fur Physikalische Chemie-Abteilung a-Chemische Thermodynamik Kinetik Elektrochemie Eigenschaftslehre 163 (1933) 378.

[66] C. T. O'Konski, J. Phys. Chem. 64 (1960) 605.
[67] J. M. Schurr, J. Phys. Chem. 68 (1964) 2407.
[68] S. S. Dukhin, V. N. Shilov, Dielectric phenomena and the double layer in disperse systems and polyelectrolytes, Wiley, New York, 1974.
[69] E. H. B. Delacey, L. R. White, Journal of the Chemical Society-Faraday Transactions II 77 (1981) 2007.
[70] C. S. Mangelsdorf, L. R. White, Journal of the Chemical Society-Faraday Transactions 93 (1997) 3145.
[71] J. Kijlstra, H. P. Vanleeuwen, J. Lyklema, J Chem Soc Faraday T 88 (1992) 3441.
[72] M. Fixman, J. Chem. Phys. 72 (1980) 5177.
[73] R. J. Hill, D. A. Saville, W. B. Russel, J. Colloid Interface Sci. 263 (2003) 478.
[74] R. J. Hill, D. A. Saville, W. B. Russel, J. Colloid Interface Sci. 268 (2003) 230.
[75] J. J. Lopez-Garcia, C. Grosse, J. Horno, J. Colloid Interface Sci. 265 (2003) 341.
[76] B. H. Bradshaw-Hajek, S. J. Miklavcic, L. R. White, Langmuir 24 (2008) 4512.
[77] S. Ahualli, A. Delgado, S. J. Miklavcic, L. R. White, Langmuir 22 (2006) 7041.
[78] F. Carrique, L. Zurita, A. V. Delgado, Colloids and Surfaces a-Physicochemical and Engineering Aspects 92 (1994) 9.
[79] L. A. Rosen, D. A. Saville, Langmuir 7 (1991) 36.
[80] F. Carrique, L. Zurita, A. V. Delgado, J. Colloid Interface Sci. 166 (1994) 128.
[81] L. A. Rosen, D. A. Saville, J. Colloid Interface Sci. 140 (1990) 82.
[82] D. F. Myers, D. A. Saville, J. Colloid Interface Sci. 131 (1989) 461.
[83] A. V. Delgado, F. Gonzalez-Caballero, F. J. Arroyo, F. Carrique, S. S. Dukhin, I. A. Razilov, Colloids and Surfaces a-Physicochemical and Engineering Aspects 131 (1998) 95.
[84] L. A. Rosen, J. C. Baygents, D. A. Saville, J. Chem. Phys. 98 (1993) 4183.
[85] M. Minor, H. P. van Leeuwen, J. Lyklema, J. Colloid Interface Sci. 206 (1998) 397.
[86] J. Kijlstra, H. P. Vanleeuwen, J. Lyklema, Langmuir 9 (1993) 1625.
[87] G. S. Manning, Biophys Chem 9 (1978) 65.
[88] F. Bordi, C. Cametti, R. H. Colby, Journal of Physics-Condensed Matter 16 (2004) R1423.

[89] H. P. Schwan, Determination of biological impedances, Physical Techniques in Biological Research, Academic Press, New York, 1963.
[90] M. M. Springer, Ph.D. Thesis, Wageningen University, 1979.
[91] C. Grosse, M. Tirado, Ieee Transactions on Instrumentation and Measurement 50 (2001) 1329.
[92] C. Grosse, M. C. Tirado, J. Non-Cryst. Solids 305 (2002) 386.
[93] J. Blom, Journal of Physics E-Scientific Instruments 12 (1979) 889.
[94] M. M. Springer, A. Korteweg, J. Lyklema, J. Electroanal. Chem. 153 (1983) 55.
[95] P. Wang, A. Anderko, Fluid Phase Equilib. 186 (2001) 103.
[96] K. S. Cole, R. H. Cole, J. Chem. Phys. 9 (1941) 341.
[97] J. Lyklema, S. S. Dukhin, V. N. Shilov, J. Electroanal. Chem. 143 (1983) 1.
[98] J. Lyklema, M. M. Springer, V. N. Shilov, S. S. Dukhin, J. Electroanal. Chem. 198 (1986) 19.
[99] B.-M. Wilén, K. Keiding, P. H. Nielsen, Water Res. 34 (2000) 3933.
[100] V. Legrand, D. Hourdet, R. Audebert, D. Snidaro, Water Res. 32 (1998) 3662.

List of supporting papers

I. Christensen, P. V. and Keiding, K., The use of dielectric spectroscopy for the characterisation of polymer-induced flocculation of polystyrene particles, Journal of Colloid and Interface Science (2008), 327, 362-369.

II. Christensen, P. V., Hinge M. and Keiding, K., The use of dielectric spectroscopy in the investigation of the effect of polymer choice on the flocculation of polystyrene particles, Journal of Colloid and Interface Science (2009), 331, 113-121.

III. Christensen, P. V., Christensen M. L. and Keiding, K., The use of dielectric spectroscopy for the characterisation of polymer-induced flocculation of core-shell particles, not submitted.

IV. Christensen, P. V. and Keiding, K., The use of dielectric spectroscopy for the characterisation of the precipitation of hydrophobically modified poly(acrylic-acid) with divalent barium ions, not submitted.

Publications not included in the thesis

I. Hjorth, M., Christensen, M. L. and Christensen, P. V., Flocculation, coagulation, and precipitation of manure affecting three separation techniques, Bioresource Technology (2008), 99, 8598-8604.